



Acenes Beyond Organic Electronics: Sensing of Singlet Oxygen and Stimuli-Responsive Materials

Journal:	<i>Organic & Biomolecular Chemistry</i>
Manuscript ID	OB-REV-08-2020-001744.R2
Article Type:	Review Article
Date Submitted by the Author:	25-Oct-2020
Complete List of Authors:	Brega, Valentina; Tufts University, Chemistry Yan, Yu; Tufts University, Chemistry Thomas, Samuel; Tufts University, Chemistry

ARTICLE

Acenes Beyond Organic Electronics: Sensing of Singlet Oxygen and Stimuli-Responsive Materials

Valentina Brega, Yu Yan and Samuel W. Thomas, III*

Received 00th January 20xx,
Accepted 00th January 20xx

DOI: 10.1039/x0xx00000x

The spectroscopic, electronic, and geometrical properties of acenes have enabled their broad applicability in organic optoelectronics, such as field-effect transistors. Beyond these physical characteristics of acenes, acenes also offer characteristic and predictable reaction chemistry, especially their behavior as dienes in cycloaddition reactions. Although these cycloaddition reactions, especially those with singlet oxygen ($^1\text{O}_2$) as the dienophile, are detrimental for organic electronics, this reactivity has led to several different applications such as sensing of $^1\text{O}_2$, the release of cytotoxic reactive oxygen species (ROS), and stimuli-responsive materials for drug delivery. The rational design of acenes in these chemically-responsive applications beyond organic optoelectronics requires an understanding of how chemical structure influences both the physical properties, such as quantum yield of emission, as well as the reactivity of acenes and their cycloadducts. Therefore, the objective of this review is to summarize how cycloaddition reactions of acenes have expanded their applications in different areas of materials chemistry, and in doing so inspire and inform the rational design of acene-based materials with applications beyond organic electronics.

1. Introduction and scope

Design of materials and cycloadditions of acenes

The rational design of organic materials relies on the possibility of programming materials based on the properties of each component. Among organic compounds, acenes are a family of molecules with predictable and programmable chemical, crystallographic,¹ and photophysical properties. Their highly conjugated, extended aromatic frameworks impart a wide range of spectroscopic and electrochemical properties amenable to the transport of excited states and charge carriers. Furthermore, the addition of substituents to the acene core, or the perturbation of the parent acene backbones with heteroarenes, allows fine-tuning of their electronic structure, and therefore of these physical properties, such that their optical spectra and HOMO-LUMO gaps cover the entire visible spectrum.² Because of their rich optoelectronic properties, acene derivatives are components of a variety of devices such as organic field-effect transistors (OFETs).³

In designing the physical properties of acenes key to their applications in optoelectronics, chemical reactions of acenes are typically detrimental to performance, decreasing stability and reliability of acenes as active materials. Nevertheless, acenes present chemical reactions that find important utility. Key to the trends of their reactivity is that their per-ring

aromatic stabilization decreases as the number of 1-D fused rings in an acene increases, resulting in the overall trend that longer acenes react faster than shorter acenes. Moreover, the enthalpic penalty for disrupting aromaticity of a single arene ring in an acene is smaller for interior rings of acenes, rendering these positions more reactive. Using anthracene as an exemplar of this regioselectivity, reactions at the 9- and 10-positions leave two benzene rings as the aromatic portions of the product, which together have a larger resonance energy than the naphthalene that would result from reaction at one of the outer rings. Acenes undergo electrophilic substitution reactions such as halo-de-hydrogenation, with substitution at the 9- and 10-positions of anthracene occurring faster than other locations. As the focus of this review, acenes undergo thermal [4+2] and photochemical [4+4] cycloaddition reactions, with anthracene again highly favoring reactions at the central ring. While it is true that cycloadditions of acenes disrupt aromaticity and are detrimental to optoelectronic devices—especially photochemical oxidation reactions—these convenient reactions are often rapid and proceed without byproducts. They have therefore yielded applications in responsive materials, such as crosslinking and grafting to surfaces, sensing of singlet oxygen ($^1\text{O}_2$), and drug delivery systems (Figure 1).

The objective of this review is to summarize and place into context the [4+2] and [4+4] cycloaddition reactions of acenes and some of their applications in materials chemistry. Depending on the structures of the acenes, their reaction partners, and the conditions used, these reactions can be either reversible or irreversible. It is important to note that this review does not cover the design of acenes for applications in organic electronics, including OLEDs and organic transistors, which has been discussed in a number of review articles.^{4,5} Similarly the

^a Department of Chemistry, Tufts University, 62 Talbot Avenue, Medford, Massachusetts 02155, United States. E-mail: sam.thomas@tufts.edu

[†] Footnotes relating to the title and/or authors should appear here.

Electronic Supplementary Information (ESI) available: [details of any supplementary information available should be included here]. See DOI: 10.1039/x0xx00000x

role of acenes in singlet fission and the fabrication of photovoltaic devices is also outside the scope of our review—we suggest here several excellent reviews on this important topic, which further bolster the continuing importance of acenes across organic materials chemistry.^{6,7} Finally, we focus this paper on acenes containing only fused benzene rings and some heteroacenes that contain fused thiophenes; for example, we do not discuss here azaacenes, which have not only been extensively discussed elsewhere,^{8,9} but are generally less reactive due to their electron-deficient nature, making them strong electron accepting materials in organic electronics.

In section 2, we summarize some common approaches and more recent developments in the synthesis of acenes, as well as their spectroscopic properties. Section 3 describes the cycloaddition reactions of acenes in carbon-carbon bond formation for stimuli responsive materials. These reactions include the [4+2] cycloadditions of acenes with some common, reactive dieneophiles, as well as photochemical [4+4] “butterfly” dimerization reactions. Given that cycloadditions with singlet oxygen to form endoperoxides are nearly ubiquitous reactions of acenes—whether such reactions are intended or to be prevented—the remainder of the review article focuses on this reaction. Section 4 describes some structure-property relationships of acene cycloadditions with singlet oxygen. Acene derivatives are commonly integrated in the design of singlet oxygen sensors, and so we describe in section 5 acene-based singlet oxygen sensors and examine their mechanism of action. Singlet oxygen probes in general, regardless of their chemical structure, have been discussed in a recent comprehensive review article.¹⁰ Acene endoperoxides that result from these reactions can cyclorevert, releasing singlet oxygen—section 6 discusses the application of such reactions in photodynamic therapy (PDT). Finally, acene endoperoxides can undergo cleavage reactions to yield degradable materials, which makes acenes increasingly popular for drug delivery applications, as described in section 7.

Cycloadditions of Acenes

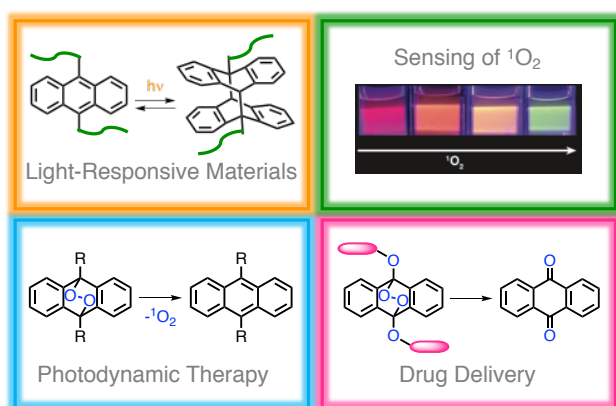


Figure 1. Schematic representation of applications of cycloadditions of acenes, including materials for sensing of singlet oxygen, drug delivery, photodynamic therapy and light-responsive materials. Adapted with permission from ref. 121. Copyright 2018 Wiley-VCH.

2. Synthesis of Acenes

Acenes comprise linearly fused benzene rings that can be considered as 1-dimensional fragments of graphene. The resulting extended conjugated structure and possibility for favorable packing motifs in the solid-state have rendered acenes as one of the most promising classes of compounds for OFETs.¹¹ It is also reported that increasing the length of acenes can improve the performance of the materials. However, due to their high HOMO levels and lower per-ring resonance energies, longer acenes can suffer from poor stability, especially during photoirradiation. This challenge around stability has resulted in a wide variety of strategies that harness substituent effects to suppress their undesirable reactivity. On the other hand, the generally increased reactivity of longer acenes could open possibilities for responsive materials. Overall, however, regardless of the intended application space, the preparation of acenes longer than anthracene can be a challenge, usually requiring sophisticated synthetic technologies.⁴

Synthesis of pristine acenes

Although the instability and lack of solubility of longer acenes are problematic in terms of quantitative synthesis, various novel strategies for their synthesis have emerged in recent years.^{12,13} In addition to notable successes in pursuit of the preparation of longer unsubstituted acenes, such as on-surface synthesis¹⁴ or rapid sequential reduction of pentacenedione,¹⁵ thermal- or photo-induced elimination reactions of acene precursors have been studied extensively. In 2007, Chow's group reported a synthetic method for the preparation of pentacene by thermal-induced extrusion of a unit of carbon monoxide.¹⁶ This reaction was carried out at 150 °C, which is much lower than the decomposition temperature of pentacene (~360 °C). Also, the higher solubility of the precursor allowed solution processing for device fabrication. Finally, the transition to pentacene was achieved by annealing. In addition, thermal elimination avoids exposure to direct light irradiation which can degrade longer acenes. Five years later, the same group reported a similar synthetic procedure for hexacene. Importantly, this work enabled thorough characterization of the optical and electronic properties of hexacene, and the authors also demonstrated the high photosensitivity of hexacene—photooxidation of the hexane thin-film occurred in minutes under UV light while the film showed no degradation in the dark for more than a month.¹⁷

Novel syntheses have also yielded unsubstituted heptacene. Bettinger and coworkers synthesized heptacene by fragmenting heptacene dimers.¹⁸ Notably, it was the first evidence of the in-bulk existence of heptacenes which was under controversy for more than 70 years.^{19,20} Moreover, the group also reported optically spectroscopic analysis of heptacene both in solution and as a vapor-deposited thin film. In an alternative approach, Jancarik and Gourdon further developed the approach of thermal decarbonylation by successfully synthesizing a series of seven-membered acenes including heptacene and non-linear dibenzopentacenes.²¹

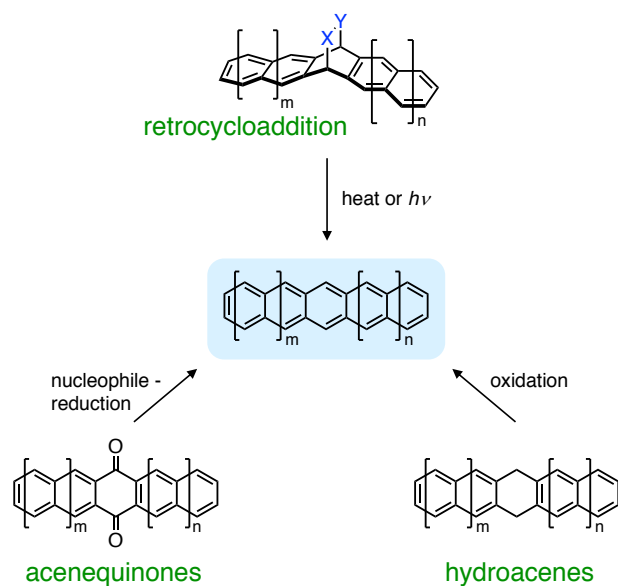


Figure 2. Common strategies of longer acene synthesis. Adapted with permission from ref. 13. Copyright (2017) Wiley-VCH.

Substituted acenes

Although numerous methodologies for synthesizing unsubstituted longer acenes have emerged, their limited solubility and stability can limit their applications. Thus, the ability to prepare functionalized longer acenes, especially those with better solubility, is crucial. As a result of these breakthroughs, the applications of longer acenes are no longer limited to the solid-state. The synthesis of stable and soluble longer acenes allows organic chemists and materials scientists to explore other potential applications both within and beyond organic electronics.

One of the most common strategies is to introduce silylethynylene substituents or other carbon-based substituents onto the conjugated acene core by addition-elimination sequences between the corresponding quinone and suitable organometallic reagents. Installation of ethynyl groups in this way can be traced back to at least 1969,²² while aryl substituents on pentacene were reported in 1942.²³ More recently, Anthony's group further developed this strategy and reported bis(triisopropylsilylethynyl)pentacene (TIPS-pentacene), a milestone material for organic electronics.²⁴ Tykwinski and coworkers reported an acid-free approach for synthesizing pentacene oligomers and the representative polymers.²⁵ Careful control over the reaction conditions can allow installation of different substituents on the acene core, yielding diversely functionalized longer acenes in recent years.^{26,27,13}

Overall, silylethynylene substituents can improve both solubility and stability of longer acenes significantly, both of which enable many of the spectroscopic analyses for acenes longer than pentacene that are commonly performed in the solution phase (Figure 3).²⁸ Further tuning of side groups can also optimize the crystal packing of the materials, thereby improving their performance in organic electronic devices.^{29,30} Supporting these

discoveries, Linker and coworkers reported in 2012 a mechanistic rationale for how triple bonds can protect the longer acenes against photooxidation.³¹ In addition, terminal alkyne substituents, which can be obtained by simple and rapid desilylation, are desirable intermediates for the Sonogashira cross-coupling reaction. Using this approach, subsequent functionalization of the ethynyl substituent on the acene could be achieved.³² For instance, our group has successfully designed and synthesized two-dimensional conjugated polymers with tetracene-based pendants.³³

More recently, Chi and coworkers reported another strategy of stabilizing longer acenes with substituent effects.³⁴ Using the Scholl reaction from diaryl-substituted pentacene, the authors obtained bisindeno-annulated pentacenes, in which the two aromatic substituents were fused onto the pentacene along their peri-positions (Scheme 1 Top). Thus, each substitution kinetically blocked two possible sites for photooxidation, thereby stabilizing the pentacene core. Also, the five-member rings generated could serve as electron-acceptors, delocalizing the HOMO and LUMO to further stabilize the electron-rich pentacene from oxidation. To avoid the incompatibility of Scholl reactions and electron-withdrawing functional groups, Plunkett and coworkers designed an alternative synthetic pathway for annulated pentacenes (CP-PEN). The hydrogenated pentacene was used as a precursor, while aromatization was executed after the Pd-catalyzed cyclopentannulation.³⁵ In the following year, Chi's group reported the preparation of Z-shaped acene dimers connected by fused pentalene, which was effective for preparing both anthracene and tetracene dimers (Z-ANT and Z-TET). Compared with the monomers, the HOMO-LUMO gaps of the dimers narrowed dramatically as determined by UV-vis-NIR absorbance and cyclic voltammetry.³⁶ Very recently, a one-pot synthesis of benzo-/thieno-annulated tetracene was reported by Murata and coworkers: the unsymmetrically annulated tetracene was synthesized through a one-step cross-dehydrogenative-coupling between the pristine tetracene and single aromatic rings like benzene or methyl thiophene (Scheme 1 Bottom). Notably, the thiophene showed a stronger capability of suppressing unwanted photooxidation,³⁷ which was also reported by the group of Briseno in their study of photostable rubrene derivatives.³⁸

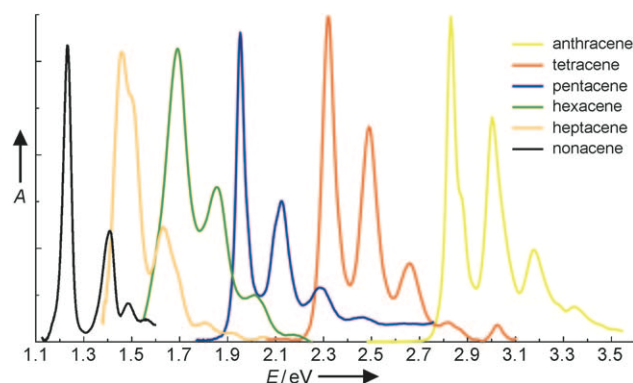
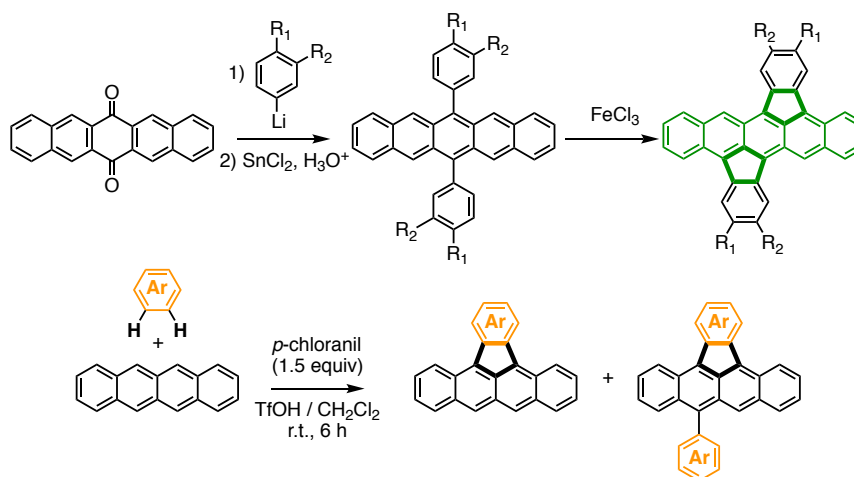


Figure 3. The absorbance spectra of silylethynylene-substituted acenes. Reproduced with permission from ref. 28. Copyright 2011 Wiley-VCH.



Scheme 1: Examples of synthesis of annulated acenes. *Top:* Synthesis of bisindeno-annulated pentacene reported by Chi and coworkers.³⁴ *Bottom:* Synthesis of benzo-/thieno-annulated tetracene reported by Murata and coworkers.³⁷

Numerous groups have made tremendous efforts to tune the frontier molecular orbital energies of larger acenes using substituent effects of electron-withdrawing groups. Beyond enhancing stability, such tuning can also improve the performance of acenes in organic electronics. For instance, Nakayama and coworkers reported the synthesis of dicyanopentacene from a bridged diol. Transistor devices containing this compound showed ambipolar activity, as opposed to the p-type hole mobility of pentacene.³⁹ Bettinger's group reported the synthesis of 2,3,9,10-tetrafluorotetracene, either by photoelimination of a diketone precursor or through a tetrazine-induced cycloreversion from bridged 6,13-ethanopentacene.⁴⁰ Finally, Agou and coworkers designed a general synthetic strategy for perfluoroalkyl (Rf) TIPS-pentacenes. The Rf groups were first introduced to a *p*-dimethylbenzene precursor followed by benzylic bromination and annulation to form Rf-substituted pentacenequinones, which were then converted to pentacenes via organolithium addition and elimination.⁴¹

Electron-donating substituents have also been recently installed onto long acenes. Ito and coworkers introduced different amino substitutions to a tetracene core. By comprehensive characterizations, the authors studied the effects of *N*-substitutions both on the geometry and the molecular orbitals, as well as the oxidation of amino groups.⁴² Our group reported a systematic synthesis of dialkoxy-substituted acenes, including thiophene-fused heteroacenes, as

well as their photo-induced cleavage reactions.⁴³ Miller's group reported water-soluble pentacenes, in which were modified by two sulfanediyl propanoic acid groups, enabling dissolution in basic aqueous solutions.⁴⁴

3. Cycloadditions of Acenes

In general, cycloaddition reactions present numerous advantages for both organic synthesis and materials science: i) they form multiple covalent bonds in one reaction, often with excellent regio- and stereoselectivity, ii) they proceed without byproduct formation, and iii) the low degree of charge separation during these reactions reduces the dependence of their rates on the polarity of the environment. In particular, acenes can react with various dienophiles due to their electron-rich nature and their diene reaction sites. In addition, acenes can also undergo photochemically allowed [4+4] "butterfly" dimerization reactions upon irradiation.⁴⁵ In this section, we will discuss both the [4+2] and [4+4] cycloaddition reactions of acenes and some recent examples of their use in organic materials. Notably, the reaction with singlet oxygen, a key reactive oxygen species, will be discussed in detail in subsequent sections.

General trends in structure-property relationships of acene cycloadditions

Grounded in basic principles of physical organic chemistry and supported by empirical data, structure-property trends for cycloaddition reactions of acenes have emerged. In general, longer acenes are more reactive than shorter acenes, as the per-ring aromatic stabilization decreases with larger number of fused rings, thereby decreasing the enthalpic penalty for disrupting aromaticity that results from replacing acene π bonds with new σ bonds. Theoretical calculations have predicted this same trend.⁴⁶ Experimentally, Ciszek's group highlighted the contribution that the lengths of acenes have on the kinetics of cycloadditions between acenes and different

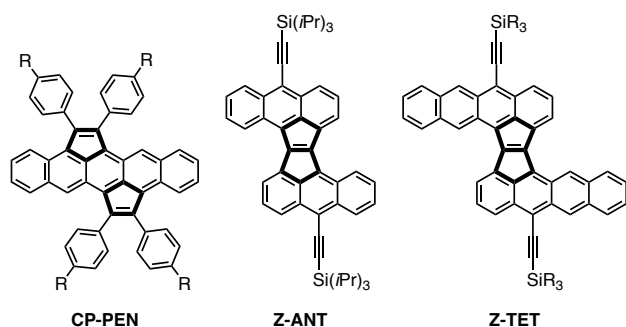


Figure 4: Chemical structures of annulated acenes reported by Plunkett³⁵ and Chi.³⁶

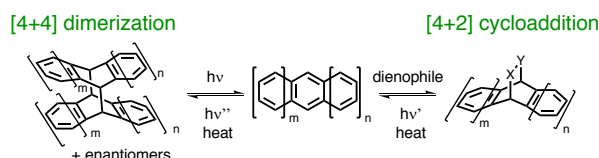


Figure 5. The [4+2] and [4+4] cycloaddition reaction of longer acenes.

reactive dienophiles such as maleic anhydride and *N*-methylmaleimide. They reported that tetracene can react nearly 100-times faster than anthracene with the same dienophile, while the reaction of pentacene was about 10-times faster than tetracene (Table 1).⁴⁷ From the perspective of regiochemistry, the interior rings of acenes—such as the 9 and 10 positions of anthracene or the 6 and 13 positions of pentacene—are generally the most reactive, usually giving excellent regioselectivity of cycloaddition at these most reactive positions. The justification of this selectivity is that the structures of these products—and presumably the structures of their transition states—preserve the greatest amount of aromatic stabilization.⁴⁸ Steric encumbrance at these sites can slow cycloaddition, as highlighted by the very slow rate of addition of many otherwise reactive dienophiles with rubrene (5,6,11,12-tetraphenyltetracene).⁴⁷

Table 1. Rate constants for cycloaddition reactions of acenes and *N*-methylmaleimide.⁴⁷

Acene	Temperature	$k_s \times 1000 \text{ (M}^{-1}\text{s}^{-1}\text{)}$
Rubrene	85 °C	0.004
Anthracene	85 °C	1.7
Tetracene	85 °C	120
Tetracene	20-25 °C	15
Pentacene	20-25 °C	110

Cycloaddition of anthracenes in materials

Due to better accessibility and stability, anthracene is a much more common intentional partner for cycloaddition reactions than longer acenes. Both [4+2] Diels-Alder reactions and photochemically promoted [4+4] dimerizations are useful in areas such as organic synthesis, post-polymerization modification, fluorescent sensing, and stimuli-responsive materials. Here we provide some recent highlights to give a sense of the breadth of possibilities, and direct readers to the excellent review of Van Damme and Du Prez for a more comprehensive summary of anthracene cycloadditions in materials.⁴⁹ The group of Swager reported an efficient synthetic strategy of complex iptycenes based on sequential mechanochemical cycloaddition of anthracenes.⁵⁰ Sumerlin and coworkers developed a new method to modify polymer architectures taking advantage of the high reactivity of anthracene in [4+2] cycloadditions. The modification was achieved via diene displacement from furan to anthracene as the anthracene could form a thermodynamically stable product.⁵¹ Berda's group reported an efficient approach for fabricating single-chain polymer nanoparticles, which used intramolecular anthracene dimerizations triggered by UV light

to fold polymer chains to an architecturally defined nanostructure.⁵² Finally, Anseth and coworkers designed an anthracene-polyethylene glycol (PEG) based hydrogel the stiffness of which could be modulated in the range of 10-50 kPa by controlling the amount of anthracene dimer formation using stepwise, low-intensity UV irradiation. The authors proposed this photochemically active material was an excellent matrix for studying mechanobiology.⁵³

In addition to unidirectional cycloadditions, the [4+4] adducts can cyclorevert, further enriching the potential of reactive anthracene-based materials. Either heating or irradiating with light of higher energy than that used for cycloaddition can yield the entropically favored fragmented products. For instance, Cong and coworkers reported thermal cleavage of anthracene dimers in the synthesis of oligoparaphenylene-derived nano hoops, demonstrating a novel strategy for obtaining a highly strained organic structure.⁵⁴ Claus and coworkers reported a new photopatterning technology based on reversible dimerization, in which a visible light LED at 420 nm induced [4+4] dimerization for writing, while UV irradiation at 360 nm induced cycloreversion and 'erasing'.⁵⁵ Chung's group developed a fluorescent sensing method for microcracks in polymer films, in which glassy poly(vinyl alcohol) (PVA) films were crosslinked by dimerization of functionalized anthracene. The cycloreversion of dimeric anthracene was triggered mechanically by crack formation, causing bright fluorescence to emerge from the resulting anthracene.⁵⁶

The reversible nature of some [4+2] acene cycloadducts is also applicable in materials. The choice of dienophiles influences the reversibility of the reaction. Lehn and coworkers have demonstrated reversible cycloadditions between a range of anthracene derivatives and the dienophile *N*-phenyl-1,2,4-triazoline-3,5-dione for application in dynamic covalent chemistry.⁵⁷ Cheng and coworkers designed polymeric micelles comprising self-assembled block copolymers linked by anthracene-maleimide adducts.⁵⁸ Rapid photo-induced

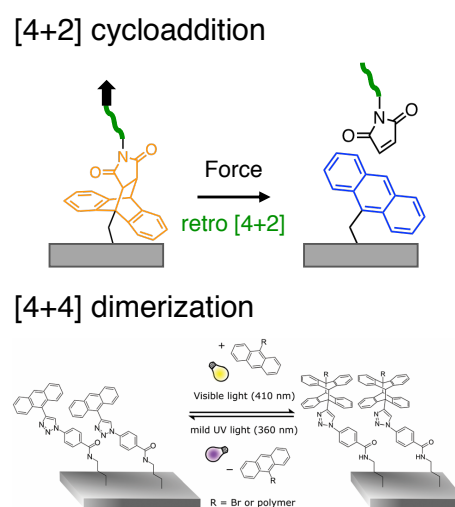


Figure 6. The application of anthracene cycloaddition in photo writing. Adapted from ref. 61. Copyright 2019 American Chemical Society and from ref. 55. with permission from The Royal Society of Chemistry.

cycloreversion of these linkers released cargo drug molecules. In addition, mechanical force can also induce cycloreversion of these bicyclic adducts. For example, Boydston's group reported the precise scission of polymer chains via retro-Diels-Alder reactions induced by sonication.⁵⁹ Subsequently, Moore and co-workers extended this mechanochemical approach to the functionalized surfaces of silica nanoparticles.⁶⁰ Moreover, in 2019, Moore, Sottos, Liu and coworkers reported spatially selective and controllable mechanophore activation on a silicon wafer. An AFM tip induced cycloreversion, enabling control over the density of activation through this readily tunable application of mechanical force.⁶¹

Cycloaddition of longer acenes

Despite their higher reactivity, only limited reports of [4+2] and [4+4] cycloadditions of longer acenes exist beyond those involving singlet oxygen (*vide infra*). We suspect that the requirements of oxygen-free conditions and more sophisticated synthesis could explain this trend. Some notable papers from the 2000s include the cycloaddition of C₆₀ and pentacene derivatives by Miller and coworkers,⁶² as well as photochemical [4+4] photodimerization of tetracene derivatives^{63,64}—while the dimerization of anthracene generally requires UV light, the dimerization of longer acenes occurs with visible light. In the last ten years, a few studies have emerged beyond the work of Ciszek discussed above. Liao and coworkers highlighted the cycloaddition between tetracene and tetracyanoethylene (TCNE) in their published work about photo-retro Diels-Alder reactions, proposing a zwitterionic intermediate structure for the photo-induced cycloreversion.⁶⁵ In the following year, the same group reported the cycloaddition of pentacene with TCNE and found a unique photo-induced two-way isomerization of the regioisomeric products in the solid-state.⁶⁶ Cheng, Lai, and coworkers reported a regioselective dimerization of tetracene derivatives in which self-assembly of side-chains yielded selective product of one out of six possible structures for tetracene dimerization.⁶⁷ Ciszek's group reported the functionalization of the surfaces of longer acene crystals via cycloaddition chemistry with different dienophiles,^{68,69} and achieved the optimization of organic/metal adhesion in flexible devices.⁷⁰ Overall, although these studies have strengthened the foundation for developing the cycloadditions of acenes longer than anthracene in functional materials, widespread implementation of these rapid reactions is still lacking.

4. Cycloaddition with singlet oxygen

Singlet Oxygen

Similar to the [4+2] cycloadditions of traditional reactive dienophiles described above, acenes undergo [4+2] cycloaddition reactions with singlet oxygen (¹O₂). ¹O₂ is an electronically excited state of dioxygen, which exists in the ground state as a triplet, and is therefore highly reactive and metastable in the singlet state. ¹O₂ is readily produced by several pathways, most simply by using photosensitization by

energy transfer from a sensitizer to O₂,⁷¹ as well as ground state chemical processes.^{72,73,10} Its low excitation energy (1.0 eV) and ease of sensitization, as well as the abundance of O₂ precursor makes ¹O₂ a common reactive oxygen species (ROS) produced upon irradiation of many chromophores in oxygenated environments. Interestingly, the lifetime of ¹O₂ depends strongly on the solvent, with coupling to X-H bonds increasing the rate of non-radiative relaxation. As a result, ¹O₂ presents the unique characteristic of substantially longer lifetimes in deuterated solvents than in the analogous hydrogenated solvents. For example, the lifetime of singlet oxygen in H₂O is 3 μs and 33-100 μs in D₂O.⁷⁴

¹O₂ participates in a wide variety of oxidative processes. It is a powerful cytotoxic oxidant that plays important roles in biologically relevant reactions, including photoinduced damage to plants and as key reactive oxygen intermediate in photodynamic therapy. Moreover, ¹O₂ undergoes characteristic reactions with organic substrates, including ene reactions with alkenes to yield organic hydroperoxides, as well as [2+2] and [4+2] cycloadditions with alkenes and dienes, respectively, to yield endoperoxides. Acenes in particular are excellent dienes for Diels-Alder reactions with ¹O₂, with many anthracene derivatives reacting with bimolecular rate constants of ca. 10⁶ M⁻¹s⁻¹. That acenes are strong chromophores with substantial excited state lifetimes can also make them good photosensitizers for ¹O₂. As a result of these two features, acenes often undergo facile "self-sensitized" endoperoxide formation, during which the acene acts both as photosensitizer for ¹O₂, as well as diene [4+2] reaction partner. This characteristic of many acenes, especially long acenes that react rapidly with ¹O₂ (*vide infra*), renders them photooxidatively unstable. While these reactions can be detrimental for organic electronics, they present applications of acenes in singlet oxygen sensing,¹⁰ drug delivery,⁷⁵⁻⁷⁸ and photodynamic therapy.⁷⁹

Kinetics of oxidation and substituent effects on reactive sites

Whether it is to exploit or ameliorate the reactions of acenes with ¹O₂, a clear understanding of how structure influences the kinetics of this oxidation reaction is critical. In general, the work of our group^{2,43} and others^{80,81,31} has demonstrated the trends of ¹O₂-acene reactivity (Figure 7) follow those of other cycloadditions described above: i) Longer acenes tend to cycloadd with ¹O₂ faster than shorter acenes with analogous substitution, with additional fused benzene rings increasing the rate more than additional fused thiophene rings. ii) Electron-releasing substituents such as alkyl groups, aryl groups, and alkoxy groups increase the rate of reaction. As an example, this impact is readily demonstrated in comparing the regioselectivity of tetracene endoperoxidations: The NMR spectrum in Figure 8 shows that for a 5,12-dialkoxytetracene (DK-TET), the endoperoxide across the electron rich substituted ring was formed in majority (90%) because of the increased reactivity of this ring compared to the unsubstituted ring. In contrast, electron-withdrawing substituents such as ethynyl

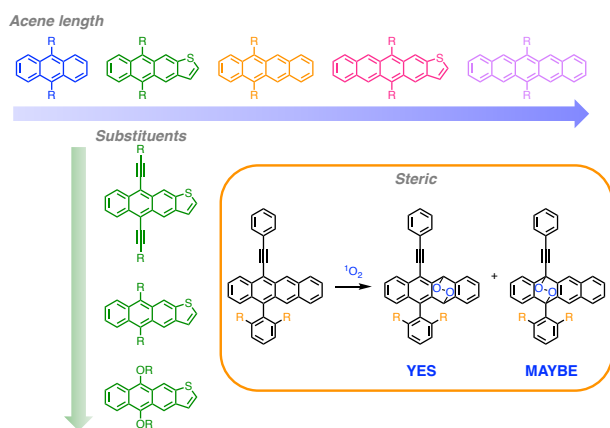


Figure 7. The reactivity of acenes toward singlet oxygen increases with the number of aromatic rings in their core. Alkynyl derivatives are the least reactive, while alkoxy derivatives reacts the fastest. Steric hindrance also plays a role in acene reactivity. Adapted with permission from ref. 84. Copyright 2015 American Chemical Society.

groups and fluorine atoms on the acene^{82,83} generally decrease the rates of endoperoxide formation.

Given the importance of long acenes in organic electronics, numerous efforts have gone into designing analogs that resist this photo-oxidation, even beyond the inclusion of electron withdrawing groups. Such efforts to improve acene photostability tend to dominate the literature regarding structure-property relationships of cycloadditions between long acenes and $^1\text{O}_2$. In these works, the small size and excited-state nature of $^1\text{O}_2$ requires unique considerations for structural designs: i. In contrast to larger dienophiles such as maleimide, the steric buttressing around the acene must be extreme to slow cycloaddition. As an example, rubrene reacts with $^1\text{O}_2$ at a rate similar to other tetracene derivatives, while 2,6-dialkylaryl substituents⁸⁴ slow endoperoxidation. Several groups, including our own,⁸⁵ have used this approach to slow the photooxidation

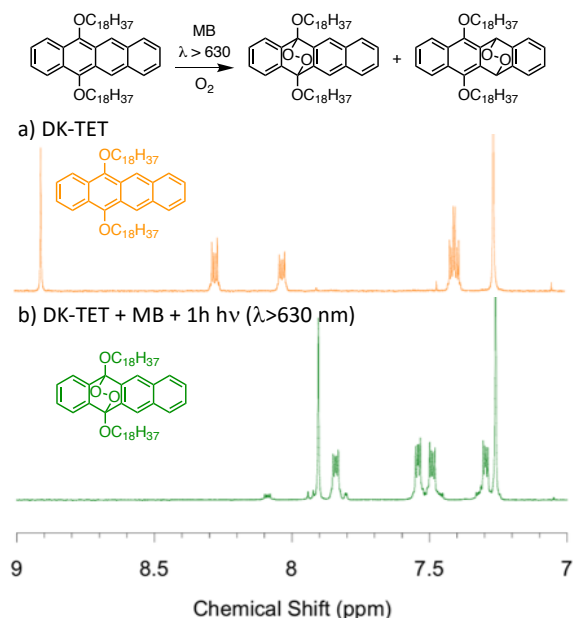


Figure 8. Substituted tetracenes yield two possible endoperoxides (5,12- and 6,11-). Dialkoxytetracene (DK-TET) react preferentially at the electron rich ring as confirmed by NMR spectroscopy (MB = methylene blue). Adapted with permission from ref. 43. Copyright 2019 Wiley-VCH.

of pentacene derivatives.^{86,81} ii. Extending acene conjugation with triple bonds can also slow cycloaddition with $^1\text{O}_2$, beyond the electron-withdrawing substituent effect. In short acenes such as anthracene, ethynyl substituents on the endoperoxide ring reduce the activation barrier to cycloreversion sufficiently such that it occurs at ambient temperature. On the other hand, long ethynylacenes such as TIPS-pentacene physically quench the electronically excited $^1\text{O}_2$, perhaps through an energy transfer mechanism, instead of adding with $^1\text{O}_2$.³¹ iii. Several reports have emerged in which the acene chemical structure renders it a poor sensitizer, rather than a poor inherent reaction partner. These include open-shell substituents on pentacene,⁸⁷ and rubrene analogs with thiophene substituents instead of phenyls.³⁸

Overall, regardless of whether the $^1\text{O}_2$ -acene cycloaddition is to be prevented or promoted, continuing to improve our understanding of how structure influences this pervasive reaction has important fundamental and applied impacts. More specifically for the purposes of this review, the $^1\text{O}_2$ cycloadditions of long acenes presents a unique combination of characteristics: i) rapid and tunable rate, ii) large changes in optical and photophysical properties as a result of the reaction, iii) the lack of byproducts in most cases, and iv) it uses only light (often visible or even near-infrared light) and O_2 as the other consumable reactants. We contend that outside of organic electronics, for which acene stability and persistence is paramount, this combination of characteristics is highly desirable for application in responsive materials.

5. Design of fluorescent materials for sensing of singlet oxygen

The combination of the rich spectroscopic properties and their fast cycloaddition reactions make acenes good probes for sensing singlet oxygen. Simple colorimetric probes typically respond with a reduction of chromophore absorbance due to interruption of conjugation after cycloaddition with $^1\text{O}_2$. As an example, 9,10-diphenylanthracene responds to $^1\text{O}_2$ where the absorbance of the band at 355 nm decreases upon reaction with $^1\text{O}_2$ with a bimolecular rate constant of $\sim 10^6 \text{ M}^{-1} \text{ s}^{-1}$.⁸⁸ Another common colorimetric probe for singlet oxygen is diphenylisobenzofuran, the initial endoperoxide cycloadduct of which cleaves to the corresponding dione. Given the importance of $^1\text{O}_2$ in biological applications, water soluble derivatives of anthracene that respond colorimetrically, such as 9,10-anthracenedipropionic acid⁸⁹ and anthracene-9,10-diyl diethyl disulfate,⁹⁰ are also known. Although they are convenient and simple, colorimetric responses for sensing applications generally offer rather poor sensitivity.

Sensing of singlet oxygen with organic fluorescent probes

Because of the higher sensitivity of luminescence spectroscopy, more recent efforts have focused on acene-based luminescent sensing schemes for $^1\text{O}_2$. Although fluorescent isobenzofuran derivatives can also respond to $^1\text{O}_2$,⁹¹ the vast majority of

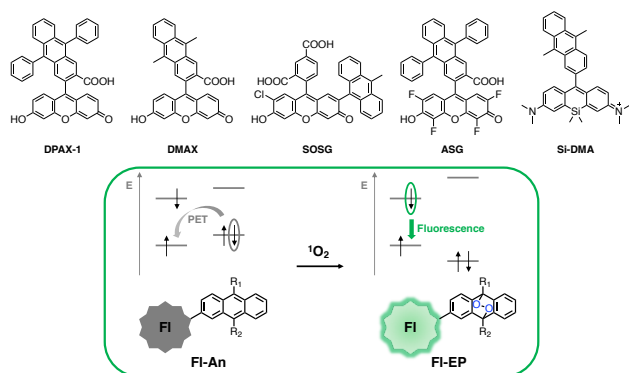


Figure 9. Top: Chemical Structure of DPAX-1, DMAX, Singlet Oxygen Sensor Green® (SOSG), Aarhus Sensor Green (ASG), Si-DMA. Bottom: Reaction of the anthracene moiety with singlet oxygen and photoinduced electron transfer (PET). Adapted from *J. Phys. Chem. B* 2013, **117**, 13985–13992. Copyright 2013 American Chemical Society.

luminescent molecular designs for sensing $^1\text{O}_2$ comprise two coupled molecular components: i) a luminescent component, such as an organic dye,⁹² a lanthanide^{93–95} or a transition metal complex,^{96–99} and ii) an anthracene derivative whose cycloaddition with $^1\text{O}_2$ changes the fate of photogenerated excited states of the luminescent component. Fluorescein derivatives feature prominently in these responsive dyes because of their high fluorescence quantum yields and solubility in water.

One of the first classes of sensors reported that pioneered this design paradigm are “turn-on” fluorophores comprising anthracenes and xanthene dyes. Before cycloaddition of $^1\text{O}_2$ with anthracene, excitation of the xanthene dye induces photoinduced electron transfer (PET) from the relatively high energy HOMO of the anthracene derivative to the dye, quenching fluorescence. After anthracene- $^1\text{O}_2$ cycloaddition, the fluorescence recovers as the interrupted conjugation of the endoperoxide decreases the energy of the HOMO, precluding electron transfer quenching. Figure 9 illustrates the general mechanism of this family of sensors and some representative chemical structures. An early and highly successful example of this design was 9-[2-(3-carboxy-9,10-dimethyl)anthryl]-6-hydroxy-3H-xanthen-3-one (DMAX), which comprises a 9,10-dimethylanthracene and xanthene fluorophore.¹⁰⁰ In an example of merging the fundamental physical organic chemistry of acene reactivity with an important application, the faster reaction of DMAX with $^1\text{O}_2$ made it more sensitive than the previously reported DPAX-1.¹⁰¹

This overall design paradigm has yielded commercially available Singlet Oxygen Sensor Green® (SOSG), which also comprises a $^1\text{O}_2$ -reactive anthracene bound to a fluorescein derivative.¹⁰² However, a primary limitation of SOSG, as is the case with many luminescent probes for $^1\text{O}_2$, remains the self-production of $^1\text{O}_2$.^{103,104} As photoexcitation of the dye is both required for fluorescent response and can lead to photosensitization, increasing background signal and/or false positives are potential pitfalls for all luminescent $^1\text{O}_2$ sensors, including SOSG. Ogilby and co-workers have addressed this challenge with their derivative Aarhus Sensor Green (ASG),

which follows a similar design paradigm, but uses a tetrafluorinated xanthene chromophore attached to a 9,10-diphenylanthracene unit.¹⁰⁵ The fluorination of the xanthene decreased the pK_a ; the resulting anionic dye is a poorer photosensitizer than the less charged, non-fluorinated version. With a similar strategy, the group of Majima designed Si-DMA, which comprised 9,10-dimethylanthracene connected to a silicon analog of rhodamine.¹⁰⁶ This turn-on sensor displayed far-red emission with a reasonable fluorescence quantum yield of 0.17.

A related design strategy includes electron rich tetrathiafulvalenes, which improve the reactivity of connected anthracenes with singlet oxygen. After reaction with singlet oxygen, the tetrathiafulvalene unit is oxidized to a radical cation, resulting in PET interruption and a chemiluminescence response.¹⁰⁷ Control experiments with other reactive oxygen species, such as hydroxyl radical, hydrogen peroxide, superoxide, and hypochlorite demonstrated that this probe is selective for singlet oxygen. The same research group has further pursued this approach, including another chemiluminescent analog containing two anthracene moieties,¹⁰⁸ as well as improved solubility in water with tetraethylene glycol pendant chains.¹⁰⁹

Beyond designs involving electron transfer quenching, anthracene derivatives have been integrated in a variety of other sensors. For example, 3,3'-(anthracene-9,10-diyl)diacrylic acid was selected as a ligand in a coordination polymer that binds tetrahedral Zinc(II) ions. In contrast to the orange fluorescence of the free ligand because of aggregation-induced emission (AIE) in ethanol/hexane mixture, the coordination polymer exhibits green fluorescence in aqueous environments, which is quenched upon cycloaddition with $^1\text{O}_2$.¹¹⁰ A $^1\text{O}_2$ sensor containing a quinolinium moiety conjugated to an anthracene undergoes a two-step cascade reaction. Initially, the fluorescence of this sensor is quenched because of intramolecular charge transfer (ICT). A first response in the blue fluorescence channel in the presence of a small concentration of $^1\text{O}_2$ (<0.6 mM) was ascribed to the cycloaddition of $^1\text{O}_2$ with the quinolinium moiety. A higher $^1\text{O}_2$ concentration (0.6–50 mM) triggered the cleavage of the anthracene and quinolinium moiety which resulted in green fluorescence.¹¹¹ Another sensing strategy involves the release of a dye covalently attached to an anthracenylmethyl unit. In this case, the endoperoxide decomposes to give anthraquinone releasing the dye molecules (fluorescein or rhodamine 6G) which yields a fluorescence turn-on response.¹¹² We discuss cleavage reactions of acenes further in Section 7.

Nanoparticles with SOSG

Given its major role in photodynamic therapy and other biological processes, sensing singlet oxygen in aqueous environments is critical but generally challenging because of the short lifetime of singlet oxygen in water and the high concentration of $^1\text{O}_2$ quenchers such as amines in biological environments. Polymer nanoparticles functionalized with acenes offer the potential for biocompatibility and modular functionalization for singlet oxygen sensing. As an example,

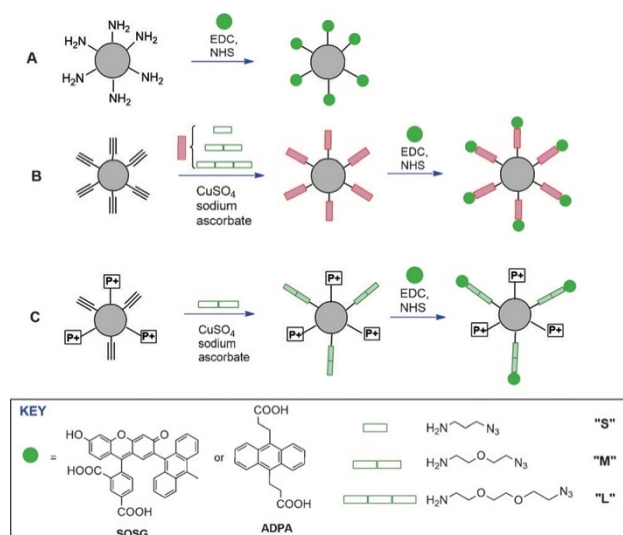


Figure 10. NanoSOSG contains polyacrylamide nanoparticles with SOSG covalently attached. Reproduced with permission from ref. 113. Copyright 2017 Wiley-VCH.

Ruiz-González and co-workers functionalized polyacrylamide nanoparticles with SOSG in different formulations. They demonstrated the versatility of this approach through direct coupling of the carboxylic acid of SOSG and the amino groups of the nanoparticles, or by adding of a spacer between the nanoparticle and SOSG to minimize interactions that can disrupt the electron transfer and increase background fluorescence (Figure 10).¹¹³ These materials were taken up by cells, and the fluorescent response of SOSG remained when bound to the nanoparticles, allowing intracellular detection of $^1\text{O}_2$. In another example of harnessing the response of SOSG in polymer nanoparticles, Wu and co-workers encapsulated SOSG into nanoparticles of the conjugated polymer poly(9,9-dioctylfluorene) (PFO).¹¹⁴ Before exposure to $^1\text{O}_2$, the nanoparticle shows the characteristic blue fluorescence of PFO as well as some background green fluorescence from SOSG, while upon exposure to $^1\text{O}_2$, the SOSG:PFO fluorescence intensity ratio increased. Therefore, the analytical readout for $^1\text{O}_2$ in this example is ratiometric (Figure 11), which can yield improved analytical figures of merit.

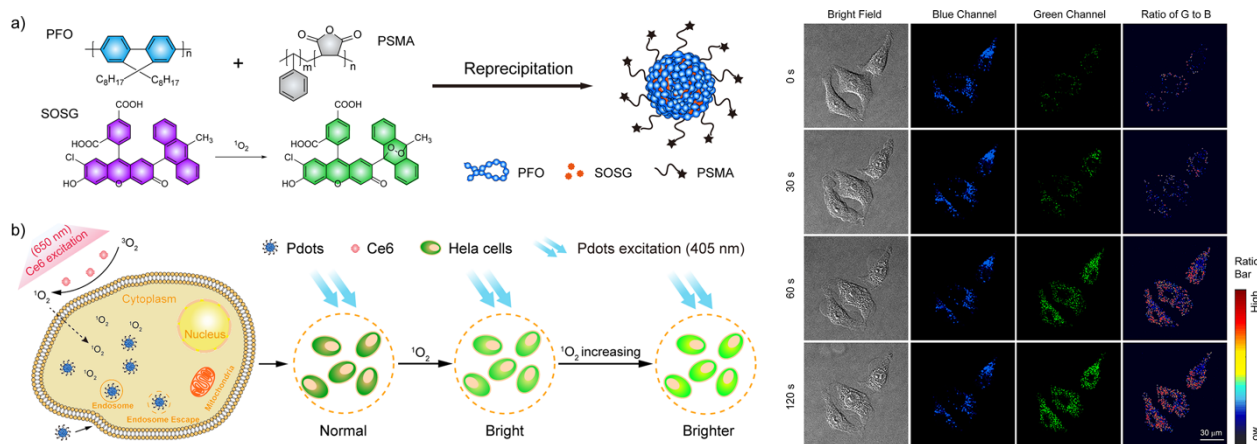


Figure 11. An example of nanoparticles with SOSG non-covalently encapsulated. Reprinted with permission from ref. 114. Copyright 2018 American Chemical Society.

Singlet oxygen sensing with longer acenes

As described in section 4, linear acenes containing more than three rings usually add $^1\text{O}_2$ faster than similarly substituted anthracene derivatives. Longer acenes therefore present two key advantages: i) they can respond faster to $^1\text{O}_2$, and ii) their more extended conjugation results in absorbance and fluorescence emission at lower energies, stretching in some cases to the red region of the visible spectrum, or even the near-infrared (NIR); the higher transmission of such wavelengths in biological environments make them ideal for imaging applications. In an effort to take advantage of these characteristics, our research group has integrated long, $^1\text{O}_2$ -reactive acenes such as tetracenes into conjugated materials with high chromophore density, which rely upon $^1\text{O}_2$ -induced changes in energy transfer. Our responsive constructs comprise a conjugated polymer as a light absorber and energy donor, while the $^1\text{O}_2$ -reactive acene is a reactive energy acceptor. Before cycloaddition, energy transfer from the conjugated polymer to the acene yields red-shifted acene fluorescence. Acene- $^1\text{O}_2$ cycloaddition and endoperoxide formation interrupts the conjugated network of the long acene, widening the HOMO-LUMO gap and preventing energy transfer, which yields blue-shifted conjugated polymer fluorescence. As a result, these materials show ratiometric fluorescent responses that blue-shift upon exposure to $^1\text{O}_2$.

Our initial effort in this area used a diaryltetracene derivative, 5,12-di(4-alkoxyphenyl)tetracene, covalently bound as a pendant side chain to a poly(fluorene-*alt*-phenylene) conjugated polymer.¹¹⁵ Energy transfer from the polymer donor to the tetracene yielded the characteristic green emission of the diaryltetracene, which shifted hypsochromically to the blue emission of the polymer backbone upon oxidation of the tetracene with photosensitized $^1\text{O}_2$. A subsequent report, described a 5,12-diethynyltetracene-linked poly(phenylene-ethynylene)s (PPE)³³ that demonstrated initial acene fluorescence enhancement upon exposure to $^1\text{O}_2$, which revealed self-quenching of the acene in the polymer. Each of these polymers displayed ratiometric responses resulting from interruption of energy transfer by $^1\text{O}_2$ -acene cycloaddition. By reducing the acene loading by 75%, the ratiometric response to

$^1\text{O}_2$ was optimized by minimizing self-quenching. In a more recent example from Nesterov and coworkers, tetracene was integrated into the backbone of a poly(arylene-vinylene) conjugated polymer as turn-on sensor for $^1\text{O}_2$.¹¹⁶

Table 2. Photophysical properties of substituted acenes.^{2,43} (DA = diaryl; DE = diethynyl; DK = dialkoxy; ANT = anthracene; AMT = anthramonothiophene; TET = tetracene; ADT = anthradithiophene; TMT = tetracenomonothiophene; PEN = pentacene)

Acene	$\lambda_{\text{max,abs}}$ (nm)	$\lambda_{\text{max,fl}}$ (nm)	Φ_f
DA-ANT	376, 263	427	0.59
DE-ANT	473, 319, 276	492	0.66
DK-ANT	385, 262	445	0.91
DA-AMT	450, 291	469	0.52
DE-AMT	520, 342, 294	538	0.75
DK-AMT	462, 278	475	0.56
DA-TET	495, 286	511	0.64
DE-TET	559, 359, 293	576	0.85
DK-TET	505, 284	522	0.49
DA-ADT	500, 308	514	0.61
DE-ADT	573, 355, 310	590	0.92
DK-ADT	518, 301	527	0.74
DA-TMT	550, 309	570	0.55
DE-TMT	615, 369, 314	634	0.64
DK-TMT	560, 303	577	0.49
DA-PEN	602, 308	620	0.09
DE-PEN	666, 377, 312	706	0.03

Acene-Doped CP Materials

Building on these approaches that incorporate long acenes into soluble conjugated polymers through covalent attachment, our group has more recently incorporated long acenes that respond to $^1\text{O}_2$ into de-solvated forms of hydrophobic conjugated polymers by doping, which does not require covalent attachment. For example, we doped thin films of poly(9,9-dialkylfluorene) with several different tetracene derivatives to yield ratiometric responses to $^1\text{O}_2$ through $^1\text{O}_2$ -induced removal of the acene energy acceptor.¹¹⁷ We found that the percentage of acene dopant is critical: in this example, films containing 2.5% (w/w) of the acene exhibited a faster ratiometric response than those with higher percentages of dopant, while lower percentages of acene dopant left the initial energy transfer process incomplete.

These energy transfer processes can also be harnessed in conjugated polymer nanoparticles (CPNs) in which the acene is non-covalently encapsulated, bypassing the need for more complex synthetic pathways. CPNs are stable colloidal suspensions in water, which can be formed by nanoprecipitation at low concentration from a water-miscible solvent such as THF. Therefore, this approach allows readily prepared, hydrophobic conjugated polymers to find a range of biological applications.^{118,119} We prepared aqueous suspensions of CPNs, using as host polymers either poly[{9,9-dioctyl-2,7-divinylene-fluorenylene}-alt-co-{2-methoxy-5-(2-ethylhexyloxy)-1,4-phenylene}] (PFPV) and poly [(9,9-dioctylfluorenyl-2,7-diyl)-alt-co-(1,4-benzo-(2,1',3)-thiadiazole)] (F8BT), doped with linear acenes containing 4 or 5 linearly fused arenes. The result is analogous to our organic-soluble

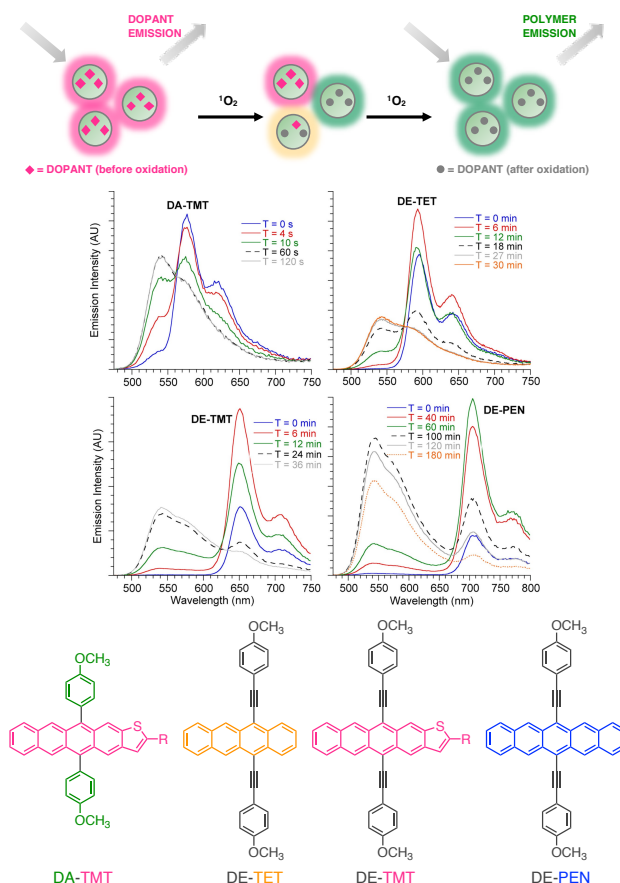


Figure 12. Top: Schematic representation of the energy transfer from a polymer donor and an acene acceptor. Middle: Fluorescent ratiometric response of CP nanoparticles. Bottom: Chemical structures of longer acenes employed in fluorescent ratiometric sensing. Adapted with permission from ref. 121. Copyright 2018 Wiley-VCH.

conjugated polymers and doped thin films: energy transfer from the polymer to the acene dopant yields red-shifted acene emission, while exposure to $^1\text{O}_2$ prepared either by irradiation of an external photosensitizer¹²⁰ or by direct irradiation of the polymer,¹²¹ decreases fluorescence of the dopant and increases that of the conjugated polymer (Figure 12). In the formulation of such CP nanoparticles, fluorescence quantum yield, absorbance spectrum, and emission maxima are key parameters: longer acenes, especially the seldom-used thienotetracenes (TMT), combine red-shifted emission with high fluorescence quantum yields. For example, the emission maximum of diethynyltetracene derivative 5,12-bis((4-methoxyphenyl)ethynyl)tetracene (DE-TET) is 576 nm with a fluorescence quantum yield of 0.85, while the emission maximum of the corresponding TMT derivative, 5,12-bis((4-methoxyphenyl)ethynyl)-2-methyltetraceno[2,3b] thiophene (DE-TMT), is 634 nm with a fluorescence quantum yield of 0.64 (Table 2).² Although pentacenes have even further red-shifted optical spectra, they often present low quantum yields of fluorescence, and unacceptably poor stability or solubility. As was the case with doped films and covalently bound polymers, the extent to which the acene is included is critical to maximizing the initial energy transfer (and therefore contrast upon exposure to $^1\text{O}_2$).

6. Reversible reactions with singlet oxygen

Release of singlet oxygen from endoperoxides of acenes

Cycloaddition reactions are often reversible at higher temperatures at which the favorable entropy of the fragmented diene and dienophile makes a larger contribution to the change in free energy. Therefore, endoperoxides can sometimes cyclorevert to yield the acenes, and potentially release $^1\text{O}_2$.⁸⁰ In a recent review article, Fudickar and Linker discussed the cycloreversion of organic peroxides, including endoperoxides of naphthalenes, anthracenes, and pyridones.¹²² In this section, we discuss only cycloreversions of acene endoperoxides that release singlet oxygen and the design of materials for photodynamic therapy comprising these endoperoxides. A prototypical example of this reaction is 1,4-dialkyl-naphthalenes. The endoperoxide can be prepared at low temperature by photosensitization; upon warming to ambient temperature, cycloreversion occurs. Due to the different spectroscopic properties of the acene and the corresponding endoperoxide, this reaction can be easily monitored by absorbance and fluorescence spectroscopy, or by following the disappearance of the UV-vis absorption band of a singlet oxygen trap molecule, such as 1,3-diphenylisobenzofuran (DPBF) or 9,10-diphenylanthracene (DPA).

As is the case for [4+2] cycloadditions, the choice of the substituents on the acene plays an important role in the kinetics of the cycloreversion reaction. For example, unfavorable non-bonding interactions between substituents appended to a naphthalene core, relieved in the rehybridized geometry of the endoperoxide, yield large steric effects for these cycloreversion reactions of naphthalenes.¹²³⁻¹²⁵ Taking advantage of the different reactivity of acenes with singlet oxygen and the reversibility of this reaction, Klaper and Linker designed a donor/acceptor system containing a 2-substituted naphthalene endoperoxide (donor) and an anthracene (acceptor) directly connected through an ester. The system transfers $^1\text{O}_2$ from the naphthalene endoperoxide to the anthracene at 315 K.¹²⁶

Linker and coworkers have also reported that endoperoxides of arylalkynylanthracenes convert to the parent acene at room temperature.^{127,31} In a different example, Fudickar and Linker executed a systematic study of three isomeric anthracenes substituted with pyridine rings at the 9 and 10-positions.¹²⁸ Unlike imidazole^{129,130} and thiophene rings¹³¹ that cause reaction with singlet oxygen, pyridines are electron-poor and render the acene more resistant to oxidation. Therefore, dipyriddylnthracenes react with $^1\text{O}_2$ 3-4 times slower than 9,10-diphenylanthracene in CH_2Cl_2 with the kinetics of oxidation depending on the position of the nitrogen atom on the pyridine ring. The *para* and *ortho* isomers react slower with $^1\text{O}_2$ than the *meta* isomer, which is ascribed to the electronic effect of the nitrogen atom. Interestingly, this reactivity order changed in less polar solvents, such as toluene or hexane, where steric effects prevail over the electronic effects. Heating the *para*- or *meta*-pyridyl endoperoxides in toluene released $^1\text{O}_2$ almost quantitatively, but the *ortho* endoperoxide did not react.

Recently, dipyriddylnthracenes have been incorporated into several designs that take advantage of endoperoxide cycloreversion and release of $^1\text{O}_2$. For example, Jakle and coworkers synthesized a series dipyriddylnthracenes that form borane complexes and can efficiently self-sensitize singlet oxygen and subsequently release it by thermal cycloreversion.^{132,133} Recently, Stang and Linker employed¹³⁴ 9,10-bis(4-pyridyl)anthracene as a building block for the self-assembly of a [6 + 6] organoplatinum(II) metallacycle (Figure 13). The corresponding endoperoxide of this complex could be prepared either by self-assembly of the ligand endoperoxide, or by conversion from the assembled acenes to the corresponding endoperoxides with $^1\text{O}_2$ produced by irradiation of the sensitizer methylene blue (MB). Regardless of the preparation method, the endoperoxide of the complex could release $^1\text{O}_2$ upon heating at 120 °C.

The clean cycloreversion of 9,10-diphenylanthracene endoperoxides allows stimuli-responsive materials that respond reversibly to photogenerated singlet oxygen. The group of Linker demonstrated the versatility of this cycloreversion reaction integrating 9,10-diphenylanthracene derivatives in the design of molecular switches where the reversible oxidation reaction controls conversion between *cis* and *trans* isomers.^{135,136} In another example of the utility of this reaction, functionalization of silicon and glass surfaces with 9,10-diphenylanthracene resulted in materials for photolithography.^{137,138} Finally, the irradiation of photochromic

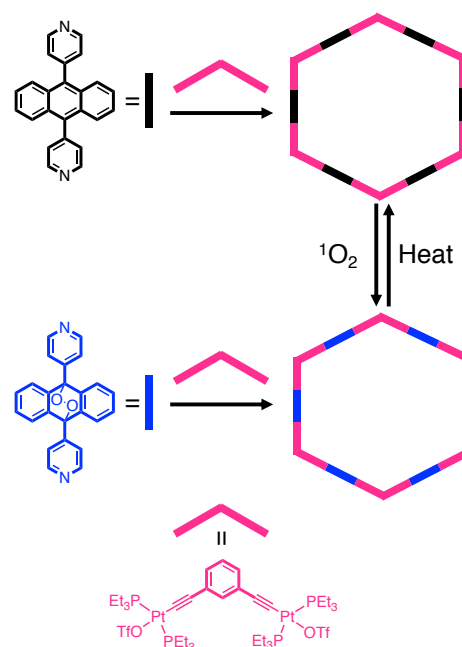


Figure 13. Design of a supramolecular complex for the release of singlet oxygen. Self-assembly of a [6 + 6] organoplatinum(II) metallacycle from 9,10-bis(4-pyridyl)anthracene and a 120° Pt(II) complex. Adapted with permission from ref. 134. Copyright 2020 American Chemical Society.

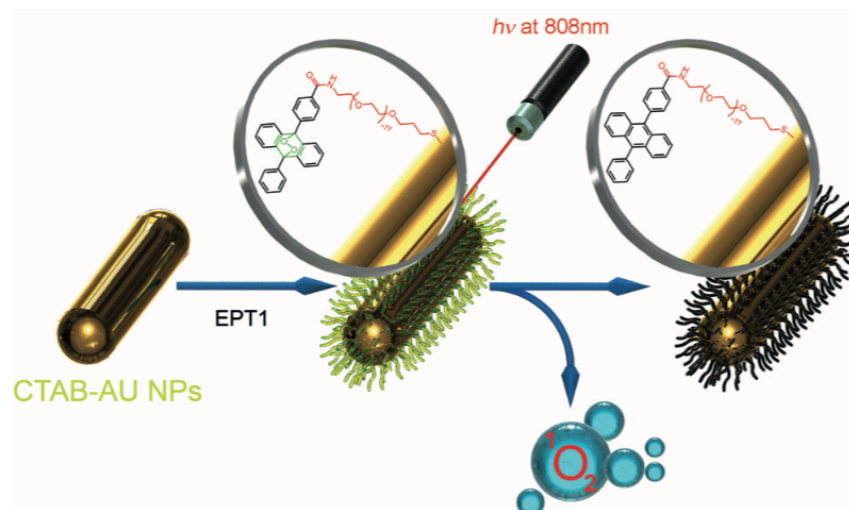


Figure 14. Release of singlet oxygen from an endoperoxide using functionalized gold nanorods for application in photodynamic therapy. Adapted with permission from ref. 79. Copyright 2016 Wiley-VCH.

thin films including a photosensitizer, tetraphenylporphyrin (TPP) or MB, and oligomeric anthracene with a photomask resulted in writing, while erasing was achieved by thermal cycloreversion.¹³⁹

9,10-Diphenylanthracene (DPA) was also selected as a building block of organic covalent cages where $^1\text{O}_2$ triggers a conformational change that affects the binding properties of polyether chains.¹⁴⁰ The conversion to endoperoxide by direct irradiation of DPA or with singlet oxygen generated by photosensitization of MB caused a change in the cavity size. The cavity of these cages accommodates one or two alkali metal ions (either Na^+ or Cs^+) depending on the cation and cavity size. The binding stoichiometry of the cages changes as a result of the change in cavity size and binding properties. Heating at 120°C resulted in endoperoxide cycloreversion to DPA and the recovery of the original cavity size. The reversible endoperoxidation of diphenylanthracene also allowed the design of luminescent supramolecular complexes that respond to light and heat. The complexation of terminal terpyridines with lanthanide ions and the reversible photooxidation of the DPA resulted in switching of the fluorescence intensity when the terpyridines are directly connected to the 9,10-diphenylanthracene core.¹⁴¹

Release of singlet oxygen for photodynamic therapy

Photodynamic therapy (PDT) is an anticancer treatment that exploits a photosensitizer and light to produce ROS, including singlet oxygen, that kills cancer cells.¹⁴² One of the challenges of photodynamic therapy for cancer treatment is the decreased concentration of oxygen in cancer cells, especially in metastatic tumors. Cycloreversion of endoperoxides has emerged as an approach to release cytotoxic singlet oxygen in low oxygen environments, with a key challenge being their compatibility with aqueous environments. Although some water soluble endoperoxides have been prepared by functionalizing naphthalene with hydrophilic groups,¹⁴³ many recent designs

involve diarylanthracene derivatives incorporated into a range of nanoparticles, polymers, or supramolecular materials. We summarize three types of examples of this approach integrating diphenylanthracenes and their endoperoxides into water-compatible materials here:

1. Diphenylanthracene endoperoxide derivatives have been tethered to gold nanoparticles¹⁴⁴ and nanorods⁷⁹ (Figure 14), which enables release of $^1\text{O}_2$ from the corresponding endoperoxides triggered by local heating upon laser irradiation at 808 nm. The efficacy of this release has been demonstrated *in vitro* by confocal microscopy of HeLa cells incubated with a ROS sensor.

2. Polymer nanoparticles containing diphenylanthracene endoperoxide have been optimized for the release of $^1\text{O}_2$ in water by emulsion polymerization of polystyrene, polyethylene glycol acrylate and polybutylmethacrylate.¹⁴⁵

3. Finally, the design of a water soluble covalent organic polymer (COP) containing a porphyrin photosensitizer and a diphenylanthracene derivative allowed photochemical production, storage, and release of $^1\text{O}_2$ through a 'catch-and-release' design.¹⁴⁶ (Figure 15) Reversible-addition-fragmentation chain transfer (RAFT) polymerization of poly(poly(ethylene glycol) methyl ether methacrylate) with a peripheral chain transfer agent enabled water-solubility. $^1\text{O}_2$, produced by irradiation of the sensitizer using red light, reacts with anthracene for 'storage', and can be released on demand by heating the COP to 110°C .

7. Irreversible reaction with singlet oxygen: acenes as cleavable linkers

Endoperoxides undergo other useful reactions besides cycloreversions. The O-O single bond is relatively weak, which can enable endoperoxide cleavage, especially under acidic conditions.¹⁴⁷ This is a productive reaction pathway for

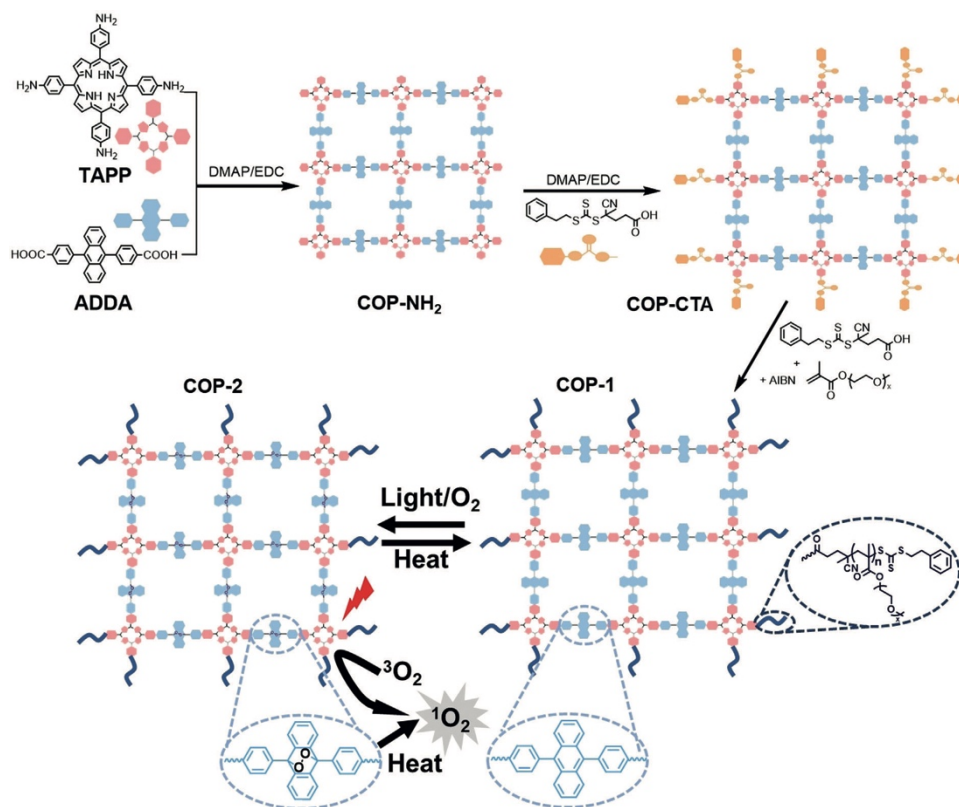


Figure 15. A covalent organic polymer (COP) prepared from a porphyrin photosensitizer and a diphenylanthracene derivative can release $^1\text{O}_2$. Reproduced with permission from ref. 146. Copyright 2020 Wiley-VCH.

application of some acenes in degradable materials and drug delivery. Base can also promote the cleavage of endoperoxides.¹⁴⁸ In particular, endoperoxides of dialkoxyacenes cleave to give alcohols and quinones,¹⁴⁷ a reactivity manifold that enables acenes to be cleavable linkers in degradable materials. The generation of singlet oxygen by photosensitization with visible light (or even near infrared light) makes this approach particularly attractive in the field of drug delivery, since these lower energy wavelengths penetrate tissue more deeply and with less cytotoxicity than higher energy wavelengths.

Examples of the cleavage reaction in responsive materials and drug delivery systems

The group of Mokhir has pioneered the use of alkoxyanthracenes in cleavable materials. In 2011, they reported the synthesis of a fluorogenic probe containing a 9,10-dialkoxyanthracene functionalized with fluorophores, in which the initial arrangement of the dyes quenches their luminescence. Subsequently, $^1\text{O}_2$ oxidizes the 9,10-dialkoxyanthracene to 9,10-anthraquinone after peroxide bond cleavage, triggering separation of the dyes and recovery of fluorescence.¹⁴⁹ Since this report, this cleavage reaction of dialkoxyanthracenes has found application in cleavable micelles,¹⁵⁰ nanoparticles,^{76,77} and supramolecular polymers.^{151,152}

We summarize here some notable examples of using this $^1\text{O}_2$ -induced cleavage of alkoxyacenes in supramolecular

materials. One example is its use in nanoparticles held together by π -stacking of anthracenes connected to a pyridinium moiety, which is encapsulated in a calixarene. Upon irradiation with UV light, the materials disassembled due to cleavage of the dialkoxyanthracene.¹⁵³ In another example, supramolecular polymers were formed by self-assembly of a 9,10-dialkoxyanthracene connected to two terminal 4,4'-bipyridinium moieties with cucurbit[8]uril (CB[8]).¹⁵² The encapsulation of two terminal 4,4'-bipyridinium units of different monomers in the cavity of CB[8] precluded the intramolecular donor-acceptor interaction with the dialkoxyanthracene, resulting in enhanced reactivity. The photooxidation and subsequent cleavage of the dialkoxyanthracene linker disassembled the supramolecular polymer as demonstrated by characterization of the anthraquinone decomposition product by NMR spectroscopy and mass spectrometry.

Similar designs of responsive materials have found applications in drug delivery systems for anticancer drugs and small interfering RNA (siRNA). The combined effect of the cytotoxicity of singlet oxygen and the triggered release of an anticancer drug yielded "enhanced" photodynamic therapy (the synergistic effect of chemotherapy and photodynamic therapy). Our group's own recent work⁷⁵ featured polymer amphiphiles containing a hydrophobic stearyl chain connected to a hydrophilic head through a cleavable linker. The polymers self-assemble into nanometric micelles that can encapsulate the anticancer agent doxorubicin in the hydrophobic core, while photoinduced cleavage of the anthracene triggers the drug

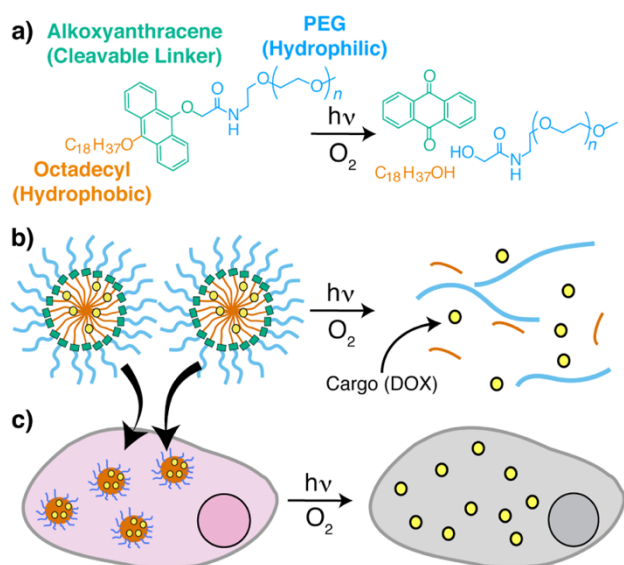


Figure 16. Self-assembly of amphiphilic polymers into micelles and intracellular delivery triggered by the cleavage reaction of the dialkoxyanthracene linker. Reprinted with permission from ref. 75. Copyright 2019 American Chemical Society.

release to realize the enhanced photodynamic therapy effect to kill HeLa cancer cells (Figure 16).

In another innovative example of harnessing alkoxyanthracene cleavage, Khashab and coworkers designed a delivery system comprising a dialkoxyanthracene connected to terminal histidines that encapsulates siRNA. Electrostatic interactions between protonated histidine and phosphate groups of siRNA yielded self-assembled spherical nanostructures. Disassembly of the nanostructures upon irradiation with green light in the presence of 1 mol% of a photosensitizer (eosin) and trifluoroacetic acid released siRNA.⁷⁸ The same group later reported the self-assembly of microtoroids that include a hydrophilic polymer (chitosan or poly(*N*-isopropylacrylamide)), iron(III) chloride, and a PEG-substituted anthracene. The anthracene cleaves upon exposure to UV light, leading the material to degrade, which allowed for templated preparation of gold and silver nanoparticles.¹⁵⁴ Finally, Mokhir and coworkers designed several related systems, including cleavable alkoxyanthracene derivatives for siRNA release,¹⁵⁵ intracellular sensing of singlet oxygen,¹⁵⁶ and detection of nucleic acids.¹⁵⁷

Although there are not many examples in this area, alkoxyacenes longer than anthracene have the potential for higher reactivity and longer wavelengths of absorbance while retaining the capability of cleaving. Our group demonstrated the cleavage of a dialkoxytetracene under irradiation ($\lambda > 420$ nm) in acidic conditions yielding tetracenequinone and stearyl alcohol (Figure 17).⁴³ Control experiments demonstrated that the endoperoxide is an intermediate of this reaction. Thus, direct irradiation of the acenes using visible light can be a useful feature in these materials, instead of relying on the more cytotoxic UV light for dialkoxyanthracene, or the inclusion of a separate photosensitizer.

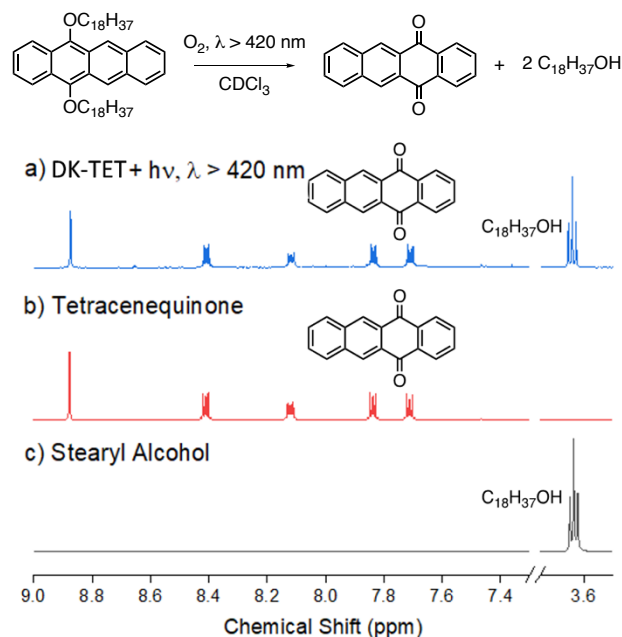


Figure 17. Acid promoted cleavage of a dialkoxytetracene (DK-TET). Tetracenequinone (b) and stearyl alcohol (c) were identified as the products. Adapted with permission from ref. 43. Copyright 2019 Wiley-VCH.

8. Conclusions and perspectives

In conclusion, we have summarized some recent developments in the [4+2] and [4+4] cycloaddition reactions of acenes, especially in the context of functional materials. Rapid and byproduct-free [4+2] cycloadditions with reactive dienophiles, including $^1\text{O}_2$, has led to the development of acene-based materials with numerous applications, such as cross-linking and ligation reactions, photopatterning processes, the sensing of $^1\text{O}_2$, and drug delivery. Many of these cycloaddition reactions are reversible, which is useful both in the synthesis of pristine acenes and in responsive materials, including the release of $^1\text{O}_2$ and the development of stimuli-responsive materials for photodynamic therapy. Irreversible reactions can trigger the disassembly of materials for drug delivery, and when combined with the cytotoxic effect of $^1\text{O}_2$, can give rise to enhanced PDT. Moreover, photochemical reactions of acenes and [4+2] cycloadditions with $^1\text{O}_2$ prepared by photosensitization allow the applications of acenes as reactive units in light-responsive materials.

Although harnessing cycloadditions of anthracenes is rather common in functional materials, similar reactions of longer acenes such as tetracene, pentacenes, and their heteroaromatic analogs in such materials are rare. Nevertheless, we contend that acenes containing four or more rings offer the advantages of faster reactivity than anthracenes as well as red-shifted optical spectra. We attribute this lack of longer acenes in reactive materials to two concerns, both of which we and others have demonstrated can be overcome: i) longer acenes are more difficult to manipulate synthetically

than anthracenes, as they generally have lower solubility and fewer commercially available functionalized precursors—however, the ever increasing variety of synthesis and substitution strategies, mainly borne out of the field of organic electronics, is allowing materials chemists to further integrate these acenes into materials either covalently or non-covalently; ii) longer acenes have a reputation for insufficient stability that make them difficult to work with—this is well deserved in some cases, and although they are usually more reactive than anthracene (giving them an advantage that we work to exploit) appropriate tuning of reactivity with substituent effects has in our experience allowed relatively straightforward handling of many derivatives. We expect that furthering our fundamental understanding of how structure can influence these properties, for anthracenes as well as longer acenes, will lead to increased attention to these compounds and reactions in the design of reactive materials.

Conflicts of interest

There are no conflicts to declare

Acknowledgements

This work was supported by the Division of Chemistry of the National Science Foundation through grant CHE-1609146.

Notes and references

- J. Jang, S. Nam, K. Im, J. Hur, S. N. Cha, J. Kim, H. B. Son, H. Suh, M. A. Loth, J. E. Anthony, J.-J. Park, C. E. Park, J. M. Kim and K. Kim, *Adv. Funct. Mater.*, 2012, **22**, 1005–1014.
- J. Zhang, Z. C. Smith and S. W. Thomas III, *J. Org. Chem.*, 2014, **79**, 10081–10093.
- J. E. Anthony, *Chem. Rev.*, 2006, **106**, 5028–5048.
- J. E. Anthony, *Angew. Chem. Int. Ed.*, 2008, **47**, 452–483.
- C. Wang, H. Dong, W. Hu, Y. Liu and D. Zhu, *Chem. Rev.*, 2012, **112**, 2208–2267.
- M. B. Smith and J. Michl, *Chem. Rev.*, 2010, **110**, 6891–6936.
- C. Hetzer, D. M. Guldi and R. R. Tykwinski, *Chem. Eur. J.*, 2018, **24**, 8245–8257.
- P.-Y. Gu, Z. Wang and Q. Zhang, *J. Mater. Chem. B*, 2016, **4**, 7060–7074.
- J. Li and Q. Zhang, *ACS Appl. Mater. Interfaces*, 2015, **7**, 28049–28062.
- Y. You, *Org. Biomol. Chem.*, 2018, **16**, 4044–4060.
- H. Sirringhaus, *Adv. Mater.*, 2014, **26**, 1319–1335.
- M. Watanabe, K.-Y. Chen, Y. J. Chang and T. J. Chow, *Acc. Chem. Res.*, 2013, **46**, 1606–1615.
- R. Dorel and A. M. Echavarren, *Eur. J. Org. Chem.*, 2017, 14–24.
- R. Zuzak, R. Dorel, M. Kolmer, M. Szymonski, S. Godlewski and A. M. Echavarren, *Angew. Chem. Int. Ed.*, 2018, **57**, 10500–10505.
- C. Pramanik and G. P. Miller, *Molecules*, 2012, **17**, 4625–4633.
- K.-Y. Chen, H.-H. Hsieh, C.-C. Wu, J.-J. Hwang and T. J. Chow, *Chem. Commun.*, 2007, 1065–1067.
- M. Watanabe, Y. J. Chang, S.-W. Liu, T.-H. Chao, K. Goto, Md. M. Islam, C.-H. Yuan, Y.-T. Tao, T. Shinmyozu and T. J. Chow, *Nat. Chem.*, 2012, **4**, 574–578.
- R. Einholz, T. Fang, R. Berger, P. Grüninger, A. Früh, T. Chassé, R. F. Fink and H. F. Bettinger, *J. Am. Chem. Soc.*, 2017, **139**, 4435–4442.
- B. Boggiano and E. Clar, *J. Chem. Soc. Resumed*, 1957, 2681–2689.
- R. Mondal, B. K. Shah and D. C. Neckers, *J. Am. Chem. Soc.*, 2006, **128**, 9612–9613.
- A. Jancarik, G. Levett and A. Gourdon, *Chem. Eur. J.*, 2019, **25**, 2366–2374.
- D. R. Maulding and B. G. Roberts, *J. Org. Chem.*, 1969, **34**, 1734–1736.
- C. F. H. Allen and A. Bell, *J. Am. Chem. Soc.*, 1942, **64**, 1253–1260.
- J. E. Anthony, J. S. Brooks, D. L. Eaton and S. R. Parkin, *J. Am. Chem. Soc.*, 2001, **123**, 9482–9483.
- D. Lehnher and R. R. Tykwinski, *Org. Lett.*, 2007, **9**, 4583–4586.
- J. L. Marshall, D. Lehnher, B. D. Lindner and R. R. Tykwinski, *ChemPlusChem*, 2017, **82**, 967–1001.
- R. R. Tykwinski, *Acc. Chem. Res.*, 2019, **52**, 2056–2069.
- B. Purushothaman, M. Bruzek, S. R. Parkin, A.-F. Miller and J. E. Anthony, *Angew. Chem. Int. Ed.*, 2011, **50**, 7013–7017.
- J. C. Sorli, Q. Ai, D. B. Granger, K. Gu, S. Parkin, K. Jarolimek, N. Telesz, J. E. Anthony, C. Risko and Y.-L. Loo, *Chem. Mater.*, 2019, **31**, 6615–6623.
- B. Purushothaman, S. R. Parkin, M. J. Kendrick, D. David, J. W. Ward, L. Yu, N. Stingelin, O. D. Jurchescu, O. Ostroverkhova and J. E. Anthony, *Chem. Commun.*, 2012, **48**, 8261–8263.
- W. Fudickar and T. Linker, *J. Am. Chem. Soc.*, 2012, **134**, 15071–15082.
- T. Iwanaga, Y. Yamamoto, K. Nishioka and S. Toyota, *Synthesis*, 2015, **47**, 3997–4007.
- E. Altinok, Z. C. Smith and S. W. Thomas III, *Macromolecules*, 2015, **48**, 6825–6831.
- A. Naibi Lakshminarayana, J. Chang, J. Luo, B. Zheng, K.-W. Huang and C. Chi, *Chem. Commun.*, 2015, **51**, 3604–3607.
- S. R. Bheemireddy, P. C. Ubaldo, P. W. Rose, A. D. Finke, J. Zhuang, L. Wang and K. N. Plunkett, *Angew. Chem. Int. Ed.*, 2015, **54**, 15762–15766.
- G. Dai, J. Chang, J. Luo, S. Dong, N. Aratani, B. Zheng, K.-W. Huang, H. Yamada and C. Chi, *Angew. Chem. Int. Ed.*, 2016, **55**, 2693–2696.
- M. Murata, M. Togo, D. Mishima, A. Harada and M. Muraoka, *Org. Lett.*, 2020, **22**, 4160–4163.
- J. Ly, K. Martin, S. Thomas, M. Yamashita, B. Yu, C. A. Pointer, H. Yamada, K. R. Carter, S. Parkin, L. Zhang, J.-L. Bredas, E. R. Young and A. L. Briseno, *J. Phys. Chem. A*, 2019, **123**, 7558–7566.
- S. Katsuta, D. Miyagi, H. Yamada, T. Okujima, S. Mori, K. Nakayama and H. Uno, *Org. Lett.*, 2011, **13**, 1454–1457.
- B. Shen, T. Geiger, R. Einholz, F. Reicherter, S. Schundelmeier, C. Maichle-Mössmer, B. Speiser and H. F. Bettinger, *J. Org. Chem.*, 2018, **83**, 3149–3158.
- T. Agou, S. Suzuki, Y. Kanno, T. Hosoya, H. Fukumoto, Y. Mizuhata, N. Tokitoh, Y. Suda, S. Furukawa, M. Saito and T. Kubota, *Tetrahedron*, 2019, **75**, 130678.
- M. Uebe, K. Kawashima and A. Ito, *Chem. Eur. J.*, 2018, **24**, 16113–16125.
- V. Brega, S. N. Kanari, C. T. Doherty, D. Che, S. A. Sharber and S. W. Thomas III, *Chem. Eur. J.*, 2019, **25**, 10400–10407.
- C. Pramanik, Y. Li, A. Singh, W. Lin, J. L. Hodgson, J. B. Briggs, S. Ellis, P. Müller, N. E. McGruer and G. P. Miller, *J. Mater. Chem. C*, 2013, **1**, 2193–2201.
- H. Bouas-Laurent, A. Castellan, J.-P. Desvergne, and R. Lapouyade, *Chem. Soc. Rev.*, 2000, **29**, 43–55.
- S. S. Zade and M. Bendikov, *J. Phys. Org. Chem.*, 2012, **25**, 452–461.

- 47 B. A. Qualizza and J. W. Ciszek, *J. Phys. Org. Chem.*, 2015, **28**, 629–634.
- 48 P. von R. Schleyer, M. Manoharan, H. Jiao and F. Stahl, *Org. Lett.*, 2001, **3**, 3643–3646.
- 49 J. Van Damme and F. Du Prez, *Prog. Polym. Sci.*, 2018, **82**, 92–119.
- 50 Y. Zhao, S. V. Rocha and T. M. Swager, *J. Am. Chem. Soc.*, 2016, **138**, 13834–13837.
- 51 H. Sun, C. P. Kabb, Y. Dai, M. R. Hill, I. Ghiviriga, A. P. Bapat and B. S. Sumerlin, *Nat. Chem.*, 2017, **9**, 817–823.
- 52 P. G. Frank, B. T. Tuten, A. Prasher, D. Chao and E. B. Berda, *Macromol. Rapid Commun.*, 2014, **35**, 249–253.
- 53 K. A. Günay, T. L. Ceccato, J. S. Silver, K. L. Bannister, O. J. Bednarski, L. A. Leinwand and K. S. Anseth, *Angew. Chem. Int. Ed.*, 2019, **58**, 9912–9916.
- 54 Z.-A. Huang, C. Chen, X.-D. Yang, X.-B. Fan, W. Zhou, C.-H. Tung, L.-Z. Wu and H. Cong, *J. Am. Chem. Soc.*, 2016, **138**, 11144–11147.
- 55 T. K. Claus, S. Telitel, A. Welle, M. Bastmeyer, A. P. Vogt, G. Delaittre and C. Barner-Kowollik, *Chem. Commun.*, 2017, **53**, 1599–1602.
- 56 Y.-K. Song, K.-H. Lee, W.-S. Hong, S.-Y. Cho, H.-C. Yu and C.-M. Chung, *J. Mater. Chem.*, 2012, **22**, 1380–1386.
- 57 N. Roy and J.-M. Lehn, *Chem. – Asian J.*, 2011, **6**, 2419–2425.
- 58 C.-C. Cheng, J.-J. Huang, A.-W. Lee, S.-Y. Huang, C.-Y. Huang and J.-Y. Lai, *ACS Appl. Bio Mater.*, 2019, **2**, 2162–2170.
- 59 D. C. Church, G. I. Peterson and A. J. Boydston, *ACS Macro Lett.*, 2014, **3**, 648–651.
- 60 J. Li, T. Shiraki, B. Hu, R. A. E. Wright, B. Zhao and J. S. Moore, *J. Am. Chem. Soc.*, 2014, **136**, 15925–15928.
- 61 A. R. Sulkanen, J. Sung, M. J. Robb, J. S. Moore, N. R. Sottos and G. Liu, *J. Am. Chem. Soc.*, 2019, **141**, 4080–4085.
- 62 G. P. Miller, J. Briggs, J. Mack, P. A. Lord, M. M. Olmstead and A. L. Balch, *Org. Lett.*, 2003, **5**, 4199–4202.
- 63 J. Reichwagen, H. Hopf, A. Del Guerso, J.-P. Desvergne and H. Bouas-Laurent, *Org. Lett.*, 2004, **6**, 1899–1902.
- 64 A. G. L. Olive, A. Del Guerso, J.-L. Pozzo, J.-P. Desvergne, J. Reichwagen and H. Hopf, *J. Phys. Org. Chem.*, 2007, **20**, 838–844.
- 65 V. K. Johns, Z. Shi, W. Dang, M. D. McInnis, Y. Weng and Y. Liao, *J. Phys. Chem. A*, 2011, **115**, 8093–8099.
- 66 V. K. Johns, Z. Shi, W. Hu, J. B. Johns, S. Zou and Y. Liao, *Eur. J. Org. Chem.*, 2012, 2707–2710.
- 67 T.-G. Hsu, H.-C. Chou, M.-J. Liang, Y.-Y. Lai and Y.-J. Cheng, *Chem. Commun.*, 2019, **55**, 381–384.
- 68 B. A. Qualizza, S. Prasad, M. P. Chiarelli and J. W. Ciszek, *Chem. Commun.*, 2013, **49**, 4495–4497.
- 69 F. Li and J. W. Ciszek, *RSC Adv.*, 2019, **9**, 26942–26948.
- 70 F. Li, J. P. Hopwood, M. M. Galey, L. M. Sanchez and J. W. Ciszek, *Chem. Commun.*, 2019, **55**, 13975–13978.
- 71 A. Greer, *Acc. Chem. Res.*, 2006, **39**, 797–804.
- 72 J.-M. Aubry and S. Bouttemy, *J. Am. Chem. Soc.*, 1997, **119**, 5286–5294.
- 73 B. F. Sels, D. E. De Vos and P. A. Jacobs, *J. Am. Chem. Soc.*, 2007, **129**, 6916–6926.
- 74 P. R. Ogilby and C. S. Foote, *J. Am. Chem. Soc.*, 1983, **105**, 3423–3430.
- 75 V. Brega, F. Scaletti, X. Zhang, L.-S. Wang, P. Li, Q. Xu, V. M. Rotello and S. W. Thomas III, *ACS Appl. Mater. Interfaces*, 2019, **11**, 2814–2820.
- 76 S. Yang, N. Li, D. Chen, X. Qi, Y. Xu, Y. Xu, Q. Xu, H. Li and J. Lu, *J. Mater. Chem. B*, 2013, **1**, 4628–4636.
- 77 S. Yang, N. Li, Z. Liu, W. Sha, D. Chen, Q. Xu and J. Lu, *Nanoscale*, 2014, **6**, 14903–14910.
- 78 S. P. Patil, B. A. Moosa, S. Alsaiani, K. Alamoudi, A. Alshamsan, A. AlMalik, K. Adil, M. Eddaoudi and N. M. Khashab, *Chem. Eur. J.*, 2016, **22**, 13789–13793.
- 79 S. Kolemen, T. Ozdemir, D. Lee, G. M. Kim, T. Karatas, J. Yoon and E. U. Akkaya, *Angew. Chem. Int. Ed.*, 2016, **55**, 3606–3610.
- 80 J.-M. Aubry, C. Pierlot, J. Rigaudy and R. Schmidt, *Acc. Chem. Res.*, 2003, **36**, 668–675.
- 81 I. Kaur, W. Jia, R. P. Kopreski, S. Selvarasah, M. R. Dokmeci, C. Pramanik, N. E. McGruer and G. P. Miller, *J. Am. Chem. Soc.*, 2008, **130**, 16274–16286.
- 82 S. Subramanian, S. K. Park, S. R. Parkin, V. Podzorov, T. N. Jackson and J. E. Anthony, *J. Am. Chem. Soc.*, 2008, **130**, 2706–2707.
- 83 M. L. Tang and Z. Bao, *Chem. Mater.*, 2011, **23**, 446–455.
- 84 R. N. Baral and S. W. Thomas III, *J. Org. Chem.*, 2015, **80**, 11086–11091.
- 85 J. Zhang, R. H. Pawle, T. E. Haas and S. W. Thomas III, *Chem. Eur. J.*, 2014, **20**, 5880–5884.
- 86 S. S. Palayangoda, R. Mondal, B. K. Shah and D. C. Neckers, *J. Org. Chem.*, 2007, **72**, 6584–6587.
- 87 A. Shimizu, A. Ito and Y. Teki, *Chem. Commun.*, 2016, **52**, 2889–2892.
- 88 F. Wilkinson, W. P. Helman and A. B. Ross, *J. Phys. Chem. Ref. Data*, 1995, **24**, 663–677.
- 89 B. A. Lindig, M. A. J. Rodgers and A. P. Schaap, *J. Am. Chem. Soc.*, 1980, **102**, 5590–5593.
- 90 P. Di Mascio and H. Sies, *J. Am. Chem. Soc.*, 1989, **111**, 2909–2914.
- 91 D. Song, S. Cho, Y. Han, Y. You and W. Nam, *Org. Lett.*, 2013, **15**, 3582–3585.
- 92 M. A. Filatov, S. Karuthedath, P. M. Polestshuk, H. Savoie, K. J. Flanagan, C. Sy, E. Sitte, M. Telitchko, F. Laquai, R. W. Boyle and M. O. Senge, *J. Am. Chem. Soc.*, 2017, **139**, 6282–6285.
- 93 B. Song, G. Wang, M. Tan and J. Yuan, *J. Am. Chem. Soc.*, 2006, **128**, 13442–13450.
- 94 B. Song, G. Wang and J. Yuan, *Chem. Commun.*, 2005, 3553–3555.
- 95 J. Sun, B. Song, Z. Ye and J. Yuan, *Inorg. Chem.*, 2015, **54**, 11660–11668.
- 96 Z. Ye, B. Song, Y. Yin, R. Zhang and J. Yuan, *Dalton Trans.*, 2013, **42**, 14380–14383.
- 97 H.-J. Yin, Y.-J. Liu, J. Gao and K.-Z. Wang, *Dalton Trans.*, 2017, **46**, 3325–3331.
- 98 Y.-J. Liu and K.-Z. Wang, *Eur. J. Inorg. Chem.*, 2008, 5214–5219.
- 99 X. Liu, P. Dai, T. Gu, Q. Wu, H. Wei, S. Liu, K. Y. Zhang and Q. Zhao, *J. Inorg. Biochem.*, 2020, **209**, 111106.
- 100 K. Tanaka, T. Miura, N. Umezawa, Y. Urano, K. Kikuchi, T. Higuchi and T. Nagano, *J. Am. Chem. Soc.*, 2001, **123**, 2530–2536.
- 101 N. Umezawa, K. Tanaka, Y. Urano, K. Kikuchi, T. Higuchi and T. Nagano, *Angew. Chem. Int. Ed.*, 1999, **38**, 2899–2901.
- 102 A. Gollmer, J. Arnbjerg, F. H. Blaikie, B. W. Pedersen, T. Breitenbach, K. Daasbjerg, M. Glasius and P. R. Ogilby, *Photochem. Photobiol.*, 2011, **87**, 671–679.
- 103 X. Ragàs, A. Jiménez-Banzo, D. Sánchez-García, X. Batllori and S. Nonell, *Chem. Commun.*, 2009, 2920–2922.
- 104 M. Marazzi, V. Besancenot, H. Gattuso, H.-P. Lassalle, S. Grandemange and A. Monari, *J. Phys. Chem. B*, 2017, **121**, 7586–7592.
- 105 S. K. Pedersen, J. Holmehave, F. H. Blaikie, A. Gollmer, T. Breitenbach, H. H. Jensen and P. R. Ogilby, *J. Org. Chem.*, 2014, **79**, 3079–3087.
- 106 S. Kim, T. Tachikawa, M. Fujitsuka and T. Majima, *J. Am. Chem. Soc.*, 2014, **136**, 11707–11715.
- 107 X. Li, G. Zhang, H. Ma, D. Zhang, J. Li and D. Zhu, *J. Am. Chem. Soc.*, 2004, **126**, 11543–11548.
- 108 G. Zhang, X. Li, H. Ma, D. Zhang, J. Li and D. Zhu, *Chem. Commun.*, 2004, 2072–2073.
- 109 X. Zheng, S. Sun, D. Zhang, H. Ma and D. Zhu, *Anal. Chim. Acta*, 2006, **575**, 62–67.

- 110 R. Dalapati, S. Nandi, K. Van Hecke and S. Biswas, *Cryst. Growth Des.*, 2019, **19**, 6388–6397.
- 111 L. Long, X. Yuan, S. Cao, Y. Han, W. Liu, Q. Chen, A. Gong and K. Wang, *Chem. Commun.*, 2019, **55**, 8462–8465.
- 112 M. Sun, S. Krishnakumar, Y. Zhang, D. Liang, X. Yang, M. W. Wong, S. Wang and D. Huang, *Sens. Actuators B Chem.*, 2018, **271**, 346–352.
- 113 R. Ruiz-González, R. Bresolí-Obach, Ò. Gulías, M. Agut, H. Savoie, R. W. Boyle, S. Nonell and F. Giuntini, *Angew. Chem. Int. Ed.*, 2017, **56**, 2885–2888.
- 114 W. Hou, Y. Yuan, Z. Sun, S. Guo, H. Dong and C. Wu, *Anal. Chem.*, 2018, **90**, 14629–14634.
- 115 J. Zhang, S. Sarrafpour, R. H. Pawle and S. W. Thomas III, *Chem. Commun.*, 2011, **47**, 3445–3447.
- 116 C.-H. Wang and E. E. Nesterov, *Chem. Commun.*, 2019, **55**, 8955–8958.
- 117 D. Koçlu, S. Sarrafpour, J. Zhang, S. Ramjattan, M. J. Panzer and S. W. Thomas III, *Chem. Commun.*, 2012, **48**, 9489–9491.
- 118 L. Feng, C. Zhu, H. Yuan, L. Liu, F. Lv and S. Wang, *Chem. Soc. Rev.*, 2013, **42**, 6620–6633.
- 119 Y. Wang, L. Feng and S. Wang, *Adv. Funct. Mater.*, 2019, **29**, 1806818.
- 120 F. Frausto and S. W. Thomas III, *ACS Appl. Mater. Interfaces*, 2017, **9**, 15768–15775.
- 121 F. Frausto and S. W. Thomas III, *ChemPhotoChem*, 2018, **2**, 632–639.
- 122 W. Fudickar and T. Linker, *ChemPhotoChem*, 2018, **2**, 548–558.
- 123 H. H. Wasserman, K. B. Wiberg, D. L. Larsen and J. Parr, *J. Org. Chem.*, 2005, **70**, 105–109.
- 124 M. Klaper and T. Linker, *Chem. Eur. J.*, 2015, **21**, 8569–8577.
- 125 E. Ucar, D. Xi, O. Seven, C. Kaya, X. Peng, W. Sun and E. U. Akkaya, *Chem. Commun.*, 2019, **55**, 13808–13811.
- 126 M. Klaper and T. Linker, *J. Am. Chem. Soc.*, 2015, **137**, 13744–13747.
- 127 W. Fudickar and T. Linker, *Chem. Eur. J.*, 2011, **17**, 13661–13664.
- 128 W. Fudickar and T. Linker, *J. Org. Chem.*, 2017, **82**, 9258–9262.
- 129 C. G. Dariva, J. F. J. Coelho and A. C. Serra, *J. Controlled Release*, 2019, **294**, 337–354.
- 130 J. Deng, F. Liu, L. Wang, Y. An, M. Gao, Z. Wang and Y. Zhao, *Biomater. Sci.*, 2019, **7**, 429–441.
- 131 M. R. Iesce, F. Cermola and F. Temussi, *Curr. Org. Chem.*, 2005, **9**, 109–139.
- 132 K. Liu, R. A. Lalancette and F. Jäkle, *J. Am. Chem. Soc.*, 2017, **139**, 18170–18173.
- 133 K. Liu, R. A. Lalancette and F. Jäkle, *J. Am. Chem. Soc.*, 2019, **141**, 7453–7462.
- 134 Y.-Q. He, W. Fudickar, J.-H. Tang, H. Wang, X. Li, J. Han, Z. Wang, M. Liu, Y.-W. Zhong, T. Linker and P. J. Stang, *J. Am. Chem. Soc.*, 2020, **142**, 2601–2608.
- 135 D. Zehm, W. Fudickar and T. Linker, *Angew. Chem. Int. Ed.*, 2007, **46**, 7689–7692.
- 136 D. Zehm, W. Fudickar, M. Hans, U. Schilde, A. Kelling and T. Linker, *Chem. – Eur. J.*, 2008, **14**, 11429–11441.
- 137 W. Fudickar, A. Fery and T. Linker, *J. Am. Chem. Soc.*, 2005, **127**, 9386–9387.
- 138 W. Fudickar and T. Linker, *Langmuir*, 2010, **26**, 4421–4428.
- 139 W. Fudickar and T. Linker, *Chem. Eur. J.*, 2006, **12**, 9276–9283.
- 140 C. Mongin, A. M. Ardoy, R. Méreau, D. M. Bassani and B. Bibal, *Chem. Sci.*, 2020, **11**, 1478–1484.
- 141 Y. Zhou, H.-Y. Zhang, Z.-Y. Zhang and Y. Liu, *J. Am. Chem. Soc.*, 2017, **139**, 7168–7171.
- 142 D. E. J. G. J. Dolmans, D. Fukumura and R. K. Jain, *Nat. Rev. Cancer*, 2003, **3**, 380–387.
- 143 D. Costa, E. Fernandes, J. L. M. Santos, D. C. G. A. Pinto, A. M. S. Silva and J. L. F. C. Lima, *Anal. Bioanal. Chem.*, 2007, **387**, 2071–2081.
- 144 A. M. Asadirad, Z. Erno and N. R. Branda, *Chem. Commun.*, 2013, **49**, 5639–5641.
- 145 S. Martins, J. P. S. Farinha, C. Baleizão and M. N. Berberan-Santos, *Chem. Commun.*, 2014, **50**, 3317–3320.
- 146 H. Lai, J. Yan, S. Liu, Q. Yang, F. Xing and P. Xiao, *Angew. Chem. Int. Ed.*, 2020, **59**, 10431–10435.
- 147 M. Bauch, M. Klaper and T. Linker, *J. Phys. Org. Chem.*, 2017, **30**, e3607.
- 148 M. Klaper, P. Wessig and T. Linker, *Chem. Commun.*, 2016, **52**, 1210–1213.
- 149 D. Arian, L. Kovbasyuk and A. Mokhir, *J. Am. Chem. Soc.*, 2011, **133**, 3972–3980.
- 150 Q. Yan, J. Hu, R. Zhou, Y. Ju, Y. Yin and J. Yuan, *Chem. Commun.*, 2012, **48**, 1913–1915.
- 151 S. Guo, X. Liu, C. Yao, C. Lu, Q. Chen, X.-Y. Hu and L. Wang, *Chem. Commun.*, 2016, **52**, 10751–10754.
- 152 T. Qian, F. Chen, Y. Chen, Y.-X. Wang and W. Hu, *Chem Commun*, 2017, **53**, 11822–11825.
- 153 Y.-X. Wang, Y.-M. Zhang and Y. Liu, *J. Am. Chem. Soc.*, 2015, **137**, 4543–4549.
- 154 S. Al-Rehili, K. Fhayli, M. A. Hammami, B. Moosa, S. Patil, D. Zhang, O. Alharbi, M. N. Hedhili, H. Möhwald and N. M. Khashab, *J. Am. Chem. Soc.*, 2017, **139**, 10232–10238.
- 155 A. Meyer and A. Mokhir, *Angew. Chem. Int. Ed.*, 2014, **53**, 12840–12843.
- 156 S. Chercheja, S. Daum, H.-G. Xu, F. Beierlein and A. Mokhir, *Org. Biomol. Chem.*, 2019, **17**, 9883–9891.
- 157 S. Dutta, A. Fülöp and A. Mokhir, *Bioconjug. Chem.*, 2013, **24**, 1533–1542.